

# An edge density definition of overlapping and weighted graph communities

Richard K. Darst,<sup>1</sup> David R. Reichman,<sup>1</sup> Peter Ronhovde,<sup>2</sup> and Zohar Nussinov<sup>2</sup>

<sup>1</sup>*Department of Chemistry, Columbia University, 3000 Broadway, New York, NY 10027, USA.*

<sup>2</sup>*Department of Physics, Washington University in St. Louis,  
Campus Box 1105, 1 Brookings Drive, St. Louis, MO 63130, USA*

Community detection in networks refers to the process of seeking strongly internally connected groups of nodes which are weakly externally connected. In this work, we introduce and study a community definition based on internal edge density. Beginning with the simple concept that edge density equals number of edges divided by maximal number of edges, we apply this definition to a variety of node and community arrangements to show that our definition yields sensible results. Our community definition is equivalent to that of the Absolute Potts Model community detection method (Phys. Rev. E 81, 046114 (2010)), and the performance of that method validates the usefulness of our definition across a wide variety of network types. We discuss how this definition can be extended to weighted, and multigraphs, and how the definition is capable of handling overlapping communities and local algorithms. We further validate our definition against the recently proposed Affiliation Graph Model (arXiv:1205.6228 [cs.SI]) and show that we can precisely solve these benchmarks. More than proposing an end-all community definition, we explain how studying the detailed properties of community definitions is important in order to validate that definitions do not have negative analytic properties. We urge that community definitions be separated from community detection algorithms and propose that community definitions be further evaluated by criteria such as these.

## I. INTRODUCTION

It is standard to use the concepts of graph theory in order to represent the interactions of complex systems. Here, the nomenclature of “nodes” and “edges” is used to represent generic items and the interactions between them[1]. One important form of structure in graph theory is that of *communities*, or strongly connected subgroups[2]. There is no single agreed upon definition for communities, but it is generally accepted that communities are groupings of nodes that are strongly connected to each other and weakly connected to nodes in other communities. It is important to note the two uses of the term “community” here. The first is a real-world grouping of objects, sometimes known as “ground-truth” in other works[3]. This grouping is not precisely mathematically defined, but is empirically defined based on the, e.g., social, anthropological, biological, etc. data upon which the graph is created[4–10]. The second form of “community” is a mathematical construction of nodes and edges. The community detection field has two goals: the definition of mathematical communities that most correspond to real-world communities, and the development of algorithms that can locate these mathematical communities within graphs.

Many community definitions have been proposed in the literature. Several reviews are dedicated to an overview and comparison of community detection (CD) methods, and more specifically, of community definitions themselves [2, 3, 11]. Often, primary emphasis is placed on the description and workings of the community detection method itself, and the method’s particular community definition is only implicitly defined as the practical result of applying the CD algorithm, and not as a separate formal definition. This has been accepted as a practical

thing to do, but much more could be learned if the scope and definitions of communities were broader.

The Girvan-Newman modularity is one of the few heavily-studied community definitions [12–16]. Modularity weights internal edges against external edges in an attempt to indicate, without any user-input parameters, a “best” community structure for any type of graph. Modularity is one of the oldest and most-emphasized of the existing community definitions, but despite its utility, there is a useful caveat to be made in the study of (ground-state) definitions of modularity. In 2006 Fortunato and Barthélemy showed that modularity has a very interesting property: namely an implicit dependence on the total size of the network to which it is applied[17, 18]. This prevents modularity-based community detection methods from resolving small communities in a large graph. In short, the optimal community in one partition of a graph depends upon properties of the graph far away. This behavior is non-intuitive and referred to as a “resolution limit.” Several attempts have been made to produce multi-resolution modularity measures which have a tunable parameter that “zooms” in or out and controls the size of detected communities [19], but these too have been shown to suffer resolution limits [20, 21]. Modularity has taught us several things. First and foremost, community definitions need theoretical study. Second, *any* global community definition may have a resolution limit, necessitating *local* community definitions [18, 20, 22, 23].

In order to understand the relevance of the work presented in this work, it is useful to look at past community detection approaches from the standpoint of optimizing over some configurational space. Instead of trying to improve sample techniques, we are looking at a different cost function which gives a *different ground state*, which

may be “more correct” than another ground state. As an example, after the introduction of modularity as a measure of community structure, many attempts were put forth to improve community detection via the use of enhanced sampling of the configuration space of community assignments in order to better optimize modularity [14, 15, 24–32]. As useful as these methods are, they all share one fundamental limit: they rely on the assumption that modularity is the correct cost function to optimize and that community detection is limited by the ability to properly sample configuration space [21]: basically, overcoming kinetic barriers in minimization dynamics. On the other hand, it is natural to place an emphasis on understanding other *ground state* community definitions and properties, i.e. the mapping from real-world to mathematical communities, before focusing on the search for optimal partitions. The viewpoint we espouse is that only after understanding ground state characteristics should one focus on the sampling required to finding that ground state. There are few such analyses in existing literature, but the number is growing.

In this work, we propose a community definition based on *internal edge density* (abbreviated as simply “edge density”). Edge density-based definitions have been considered before in a wide variety of contexts [3, 11, 33–37]. The particular edge density definition we focus on has been used in an implicit fashion previously [38, 39], but has never been explicitly defined and extensively studied, as we do here. Our definition affords us the ability to *compare* the properties of graph-based communities to the properties of real-world communities as a means of quantifying the degree to which they match. Currently the most common method of assessing community detection algorithms is to choose a test graph and run community detection. This gives a biased perspective of community detection, since it takes some initial belief about the structure of communities and optimizes methods towards that definition. Recently, there has been much needed emphasis on the comparison of community definitions to real-world communities. In order to make progress, we show how edge density relates to *actual* properties of model graphs and communities.

In addition to the above benefit of edge density-based communities, edge density can be quite naturally extended to weighted and multi-graphs, and handle overlapping communities, all important areas of modern research in community detection. In particular, few algorithms have been proposed that are capable of detecting overlapping communities. Thus, our work not only provides a conceptual breakthrough in terms of a rigorous analysis of new community definitions, but also provides a practical benefit in community detection ability. As an outgrowth of these extensions, we propose a new *variable topology Potts model*, which allows a more natural means of community detection in *heavily weighted graphs*.

To provide concrete illustration of these claims, we turn to a recently proposed social network model. In particular, we focus on recent work of Yang

and Leskovec (YL), who have proposed a new model of social networks, the *Affiliation Graph Model (AGM)*[40]. This model takes into account features observed in real-world social networks found via comparison with online social networks. YL claim that no current community detection algorithms can describe and detect communities in these graphs. We conceptually show that the edge density community definition models this graph properly, and then perform actual community detections to prove that this is the case.

We do not claim here that edge density is a universal definition of community that applies to all possible communities in all possible graphs. Instead, we provide the tools to determine if any one particular class of graphs is well described by an edge density picture, either by an analysis of the graph generation process, or properties of the edge structure. We hope to inspire similarly detailed analysis, and more rigorous comparison, of existing and future community definitions.

This remainder of this work is organized as follows: In section II, we define the basic tools needed to quantify edge density, then state our edge density definition. In section III, we describe historic and new edge density models, and the Potts model framework we use to perform actual community detection. In section IV, we describe some universal properties of edge density, which are independent of the exact model used to perform community detection. In section V, we describe how certain models handle the boundaries between communities differently, and explain our model of choice. In section VI and Appendix A, we discuss practical considerations for constructing an actual algorithm employing edge density. In section VII, we validate the use of edge density as a scale parameter. In section VIII, we discuss general considerations for overlapping communities, and contrasting with some recent work, we show that edge densities detect the correct conceptual behavior. In section IX, we rigorously correlate our edge density to affiliation graph models, and see that we can detect these communities easily. In section X, we describe the extension to weighted graphs, and how our new variable topology Potts model provides a significant improvement over older models. In section XI, we discuss various possible extensions. In section XII, we discuss some general background and address some possible limitations of edge density. In section XIII, we discuss the danger of over-optimizing to particular benchmark models and why studies of edge density are useful nonetheless. In section XIV, we provide concluding remarks and discuss directions for future research.

## II. EDGE DENSITY

We must first define the nomenclature and measures we will use. We will specify communities or groups of nodes by capital latin letters such as  $A$  and  $B$ , and individual nodes by lowercase letters such as  $a$ ,  $b$ ,  $x$ , and  $y$ . In

particular, the node  $a$  shall represent an arbitrary node of community  $A$ , and specific nodes of community  $A$  are indexed as  $a_i$ . The nodes  $x$  and  $y$  generally represent nodes which are not currently in any community. The community  $A$  will have  $n_A$  nodes.

We use a set terminology to discuss communities and groups of nodes. Set union is denoted with “ $\cup$ ”, indicating every node on the left or right or both sides of the operator. Set intersection is denoted “ $\cap$ ”, indicating every node that is on both sides of this operator. We use this nomenclature loosely, allowing constructs such as “ $A \cup x$ ” even though we are operating on a community on the left and an individual node on the right. This should be taken to mean union of the set of nodes in community  $A$  and the set of nodes containing  $x$ .

For any group of nodes (explained below),  $l$  represents the maximal number of possible edges (“links” in our nomenclature). The variable  $e$  represents the actual number of edges. The *edge density*  $\rho$  is the fraction of these links which have edges actually present,

$$\rho = \frac{e}{l}. \quad (1)$$

We can calculate the edge density within and between a variety of different types of groupings of nodes, all of which can be useful under different circumstances. Fig. 1 illustrates the most common situations. (a) We can calculate the edge density within only one community  $A$ , in which case  $l = \frac{1}{2}n_A(n_A - 1)$ . Community edge density is used to quantify the absolute community size and scale. (b) We can calculate the edge density between a community  $B$  and a node  $x$  not currently in community  $B$ , in which case  $l = n_B$ , since that node can connect once to every node in  $B$ . This is useful when deciding if a node should enter or leave a community. (c) We can calculate the edge density between two communities  $C$  and  $C'$ , in which case  $l = n_C n_{C'}$ , since every node in  $C$  can connect once to every node in  $C'$ . This is useful when testing if two communities should merge. (d) We can calculate the edge density for the case of one node  $y$  which has edges between two communities  $D$  and  $D'$ , in which case  $l_{By} = n_B$  and  $l_{D'y} = n_{D'}$ . This is useful for deciding which of two communities the node  $y$  would prefer to join. (e) By convention, when we calculate the edge density between a community  $E$  and node  $e'$  which is currently within that community, we only consider links between  $e'$  and the  $n_E - 1$  other nodes of the communities. Thus, in this case,  $l_{Ee'} = n_E - 1$  instead of  $n_E$ , in contrast to case (b).

### A. The edge density community definition

The most basic form of an edge density community definition (EDCD) for overlapping or isolated communities consists of three parts. (a) A community  $A$  of scale  $\rho^*$  is a *subset of nodes with an internal edge density  $\rho_A$  greater than  $\rho^*$* . (b) Communities are taken to be as large

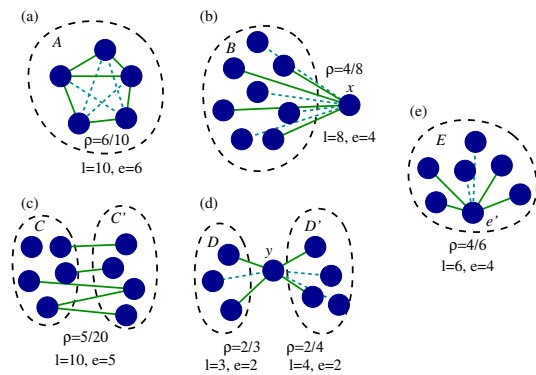


FIG. 1: Edge density calculations in a variety of situations. For each situation,  $l$  is the maximal possible number of edges,  $e$  is the actual number of edges, and the edge density  $\rho = e/l$ . In (a), we see the edge density of one community  $A$ , a group of  $n = 5$  nodes, with  $l = \frac{1}{2}n(n - 1) = 10$  total possible links (dotted and solid lines),  $e = 6$  actual edges (solid lines), thus leading to a  $\rho_A = \frac{6}{10}$ . In (b), we see the edge density definition applied between one node  $x$  and a community  $B$ . The community  $B$  contains eight nodes, for a total number of possible links to node  $x$  of  $l_{Bx} = 8$ . We see four actual links in place, leading to a  $\rho_{Bx} = \frac{4}{8}$ . Note that the internal connectivity of the community  $B$  is irrelevant and not shown. In (c), we see the edge density as applied to two communities  $C$  (5 nodes) and  $C'$  (4 nodes). Internal edge structure is again irrelevant and not shown. There are a total of  $l_{CC'} = n_C n_{C'} = 20$  possible links between these two communities,  $e_{CC'} = 5$  edges in place, for an edge density of  $\rho_{CC'} = \frac{5}{20}$ . (d) shows the edge density of one node  $d$  being pulled between two communities  $D$  and  $D'$ . Edge density for each half is in analogy to (b). In (e), we see the edge density between a node  $e$  and a community which contains it,  $E$ . This is similar to (b) except that, by convention, we use  $n_E - 1$  links as our basis.

as possible (absorbing as many nodes as possible) as long as  $\rho > \rho^*$ . (c) A community  $A$  of scale  $\rho^*$  must have each individual node  $a$ 's edge density  $\rho_{Aa} > \rho^*$ .

Part (a) is the essence of the definition, establishing a scale parameter of the communities. Part (b) is necessary because without it, we could always prefer smaller, more dense communities. For example, a graph could be partitioned into two-node cliques, all of which have an edge between the nodes, to get communities which all have  $\rho = 1$  but do not provide useful information concerning the overall structure of the graph. Part (c) is necessary to ensure that every node is well-connected to the community, preventing nodes only loosely connected from being added to any community. In future sections, we will rigorously show that the absolute Potts model and the variable topology Potts model return communities satisfying these criteria. Part (a) will be shown via Eqs. (11, 18) in Sec. III. Parts (b) and (c) are discussed in Sec. IIID.

This definition is sufficient when communities are considered in isolation, i.e. when we never consider one node and must decide which of several communities it might

join, if it would increase  $\rho$  for any of them (Fig. 1 (d)). In these cases, one may choose to add the node to a larger community resulting in a still larger resultant community, or to the community to which it shares the higher edge density. Both of these are reasonable options. One simple criteria would be to use the total number of edges as a criteria: a node  $x$  joins community  $A$  instead of community  $B$  if  $e_{Ax} > e_{Bx}$ . Existing edge density community definition methods make different choices here, which will be discussed in Section V.

### B. Connection to graph generation processes

The edge density variable  $\rho$  refers to actual edge densities in a specific graph instance. Many benchmark graphs are designed stochastically, with edges placed within or between communities with a some specified probability of  $p$ . Since each link (possible edge) has an edge placed with a probability of  $p$  independent of all other edges, the variable  $e$  (number of edges placed) is binomially distributed with mean  $lp$  (and probability of success  $p$ ). Each of the situations depicted in Fig. 1 can have a defined  $p$ . For example, *planted  $l$ -partition model* (also known as *Stochastic Block Models* (SBMs)) graphs are defined by specifying intra-community edge densities  $p_A, p_B$ , etc. (Fig. 1 (a)), and inter-community edge densities  $p_{AB}, p_{AC}, p_{BC}$ , etc. (Fig. 1 (c)) [41]. Then, each respective  $e$  will have a binomial distribution with (its respective)  $l$  trials and (its respective)  $p$  chance (of an edge) per trial,

$$P[e = x] = \mathcal{B}(x; l, p) \approx \mathcal{N}(x; lp, lp(1-p)). \quad (2)$$

$\mathcal{B}(l, p)$  represents a binomial distribution of  $l$  trials and  $p$  probability per trial, and  $\mathcal{N}(\langle x \rangle, \sigma^2)$  represents a normal distribution with a mean of  $\langle x \rangle$  and a variance of  $\sigma^2$  after we make a normal approximation to the binomial distribution. With  $\rho = e/l$ , we have a distribution of  $\rho$  of

$$P\left[\rho = \frac{x}{l}\right] = \mathcal{B}(x; l, p), \quad (3)$$

$$P[\rho = x] \approx \mathcal{N}\left(x; p, \frac{p(1-p)}{l}\right). \quad (4)$$

In the above, we employed the following shorthand for (a normalized) binomial distribution,

$$\mathcal{B}(m; n, p) = \binom{n}{m} p^m (1-p)^{n-m}. \quad (5)$$

The normal distribution is, explicitly, given by

$$\mathcal{N}(x; \langle x \rangle, \sigma^2) = \frac{1}{\sqrt{2\pi\sigma^2}} \exp\left[-\frac{[x - \langle x \rangle]^2}{(2\sigma^2)}\right]. \quad (6)$$

Clearly,  $\rho$  is a random variable with a mean of  $p$  and has a standard deviation of  $\sqrt{\frac{p(1-p)}{l}}$ . We see the intuitive result that as we approach larger community sizes,

we approach mean-field  $\rho = p$  with decreasing standard deviation around this mean. This relation between  $\rho$  and an underlying  $p$  is valid for any case where all links share the same edge probability.

## III. EDGE DENSITY MODELS

In the previous section, we stated a basic edge density definition. This definition has been implicitly used in several preexisting community detection methods. Thus, the edge density community definition is not new, but it has never been as explicitly stated and analyzed. Before we proceed to more specific uses of the edge density community definition, we will review existing Potts-model based edge density community definitions.

Recent edge density-based community definitions are formulated in terms of *Potts models* [42–44]. The Potts model is a spin system, with each site having one of up to  $q$  associated spin flavors  $\sigma = 0, \dots, q-1$ . It is similar to the Ising model except that the Ising model allows spins of only 0 or 1 (i.e., the Ising model is a Potts model with  $q = 2$ ). For community detection, we take the spin flavor of each site (node) as corresponding to a community assignment. That is, if  $\sigma_a = p$  then node  $a$  lies in community number  $p$ . (The index  $p$  clearly lies in the range  $0 \leq p \leq (q-1)$ ). Inter-site interactions which define a Hamiltonian are minimized to find an optimal community assignment. This may be done by penalizing inter-community edges and favoring intra-community edges. Reichardt and Bornholdt explain the balances and equivalences of sums of internal and external edges in [19]. The Reichardt-Bornholdt (RB) Potts model was the first explicit Potts model used for community detection, but it does *not* use our edge density community definition [19, 22]. Instead, the RB Potts model is equivalent to the Girvan-Newman modularity. Because the RB Potts model does not correspond to the edge density definitions in this paper, it is not considered in the following analysis.

Potts models are ideal for edge density definitions, because they consist primarily of a sum over all edges [45]. The models allow us to select only internal edges, although it is equally possible to select only external edges. One possible limitation of Potts models is that each node can only be associated with one community. This would seem to exclude the possibility of overlapping communities. In order to expand the Potts models to allow overlapping communities, we reformulate the models away from an edge-centric definition towards an equivalent community-centric definition.

### A. Absolute Potts model

The absolute Potts model (APM) is a spin-based ferromagnetic community detection method [38, 39]. It has been shown to be very accurate at community detection

under a wide variety of circumstances[38, 39, 46, 47]. The APM implicitly uses the edge density community definition. In the Potts representation of the APM, the CD problem is mapped onto an energy minimization of a Hamiltonian defined over pairs of spins

$$E = - \sum_{a,a' \neq a} \frac{1}{2} (A_{aa'} - \gamma B_{aa'}) \delta(\sigma_a, \sigma_{a'}). \quad (7)$$

The sum above is over distinct nodes  $a, a'$  with, as explained above,  $\sigma_a$  denoting the community assignment of node  $a$ , and  $A_{aa'}$  being the weighted ‘‘adjacency matrix’’. In unweighted graphs,  $A_{aa'} = 1$  if an edge is present between nodes  $a$  and  $a'$ , and  $A_{aa'} = 0$  otherwise. For weighted graphs, described further in Sec. X,  $A_{aa'} = w$ , where  $w$  is the respective edge weight. In unweighted graphs, we will define the ‘‘inverse adjacency matrix’’ to have elements of  $B_{aa'} = 1$  if there is no edge present, zero otherwise. For more general unweighted graphs, we will set  $B_{aa'} = 1 - A_{aa'}$ . In these models, lower energies are attractive, and any shifts in community assignment that lower energy are favorable.

This Hamiltonian in Eq. (7) involves a sum over all edges. However, due the presence of the Kronecker delta (i.e.,  $\delta(\sigma_a \sigma_{a'}) = 1$  if  $a = a'$  and zero otherwise), the sum is inherently local. That is, the sum contains only edges between nodes which are in the same community. An inter-community edge has a favorable (negative) energy of 1, and each missing edge has an energy penalty (positive energy) of  $\gamma$ . While typically represented within a spin formulation, this can be recast with the primary sum over communities instead of over edges:

$$E = - \sum_A \sum_{(a,a' \neq a) \in A} \frac{1}{2} (A_{aa'} - \gamma B_{aa'}), \quad (8)$$

with  $(a, a')$  being all ordered pairs of nodes in community  $A$ . By the use of the term ‘‘ordered’’, we make evident that we include both the pair  $(a, a')$  and the pair  $(a', a)$  (for  $a \neq a'$ ) in the sum. The spin formulation appears simpler conceptually, and may be implemented much more efficiently, although the community-centric definition allows us to make additional theoretical progress.

Since the inner sum of  $\frac{1}{2}A_{aa'}$  is the number of edges in community  $A$ , and the sum of  $\frac{1}{2}B_{aa'}$  is the number of missing edges in community  $A$ , we can rewrite this as

$$E = - \sum_A (e_A - \gamma(l_A - e_A)), \quad (9)$$

where the inner sum has been rewritten in terms of the number of existing edges  $e_A$  and the number of missing edges  $l_A - e_A$ . With minor rearrangement and invoking our edge density definition  $\rho = e/l$ , we may rewrite the energy in terms of edge density with a prefactor of  $l_A$ ,

$$E = - \sum_A l_A (\rho_A - \gamma(1 - \rho_A)). \quad (10)$$

The energy is now written as *sum over edge densities*. We see that for the energy of any one community to be negative (attractive and having a binding energy), the term  $\rho_A - \gamma(1 - \rho_A)$  must be positive. Rearranging, this gives us a correspondence between the APM variable  $\gamma$  and the critical (minimum) edge density  $\rho^*$

$$\rho_A > \frac{\gamma}{1 + \gamma} = \rho^*. \quad (11)$$

Eq. (11) is the fundamental relationship between the APM variable  $\gamma$  and the edge density critical value  $\rho^*$ . It shows that any community returned by the APM must satisfy the edge density community definition part (a). We can now state two identical relationships which give equivalences of the APM and the edge density viewpoints:

$$\rho^* = \frac{\gamma}{1 + \gamma}, \quad (12)$$

$$\gamma = \frac{\rho^*}{1 - \rho^*}. \quad (13)$$

We can rewrite the APM Hamiltonian in terms of  $\rho^*$  instead of  $\gamma$  using Eqs. (10, 13),

$$E = - \sum_A l_A \left( \frac{\rho_A - \rho^*}{1 - \rho^*} \right). \quad (14)$$

We can now relate the previously existing APM to our new edge density community definition. First, if  $\rho_A > \rho^*$ , the energy of community  $A$  is negative, and thus has a binding energy. Therefore, all communities  $A$  must have  $\rho_A > \rho^*$ , corresponding to the edge density community definition part (a). Second,  $1/(1 - \rho^*)$  and  $l_A = \frac{1}{2}n_A(n_A - 1)$  are scale factors. In order to minimize energy (and create the best partition according to the APM), we want  $l_A$  to be as large as possible (larger communities), and also  $\rho_A$  to be as large as possible. Furthermore, because of the factor  $(\rho_A - \rho^*)$ , increasing the edge density of the community also results in lower energy. As we will see in Sec. VII, larger community sizes generally tend to imply smaller  $\rho$ , thus larger community size and larger  $\rho$  are competing factors which must be balanced. Eq. (14) quantifies that balance. Communities with single nodes (‘‘size one’’ communities) have  $E = 0$  according to Eq. (7), and this can be represented in Eq. (14) if we define a community consisting of only one node to have  $\rho = 1$ .

## B. Variable topology Potts model

The absolute Potts model [38, 39] has, by now, been introduced and studied in earlier works. The variable topology Potts model (VTPM), which we now introduce, has been hinted at in previous literature, but never defined nor extensively analyzed[22, 48]. A somewhat similar technique was used in Ref. [47], where *weights* were

shifted by a value  $\bar{V}$ . The approach of Ref. [47] technique requires an adjustment of two variables,  $\bar{V}$  and  $\gamma$ , in order to find optimal partitions, while the technique of this section only requires adjustment of  $\rho^*$ .

The defining property of the variable topology Potts model is that it assigns a constant penalty (of size  $\rho^*$ ) to all links, as opposed to only missing edges. The VTPM Hamiltonian is

$$E = - \sum_{a,a' \neq a} \frac{1}{2} (A_{aa'} - \rho^*) \delta(\sigma_a, \sigma_{a'}). \quad (15)$$

As in the APM, this can be recast into a form which sums over communities first, instead of over all pairs of nodes

$$E = - \sum_A \sum_{(a,a' \neq a) \in A} \frac{1}{2} (A_{aa'} - \rho^*), \quad (16)$$

with all variables analogous to the APM nomenclature in Eq. (8). We proceed as in the APM to turn this into an edge-density based definition using the same relation  $e_A = \sum A_{aa'}$

$$E = - \sum_A l_A (\rho_A - \rho^*). \quad (17)$$

We, again, have a criteria which must be satisfied for any VTPM community to have a binding energy,

$$\rho_A > \rho^* \quad (18)$$

which is identical to the criteria of the APM and of edge density community definition (a). In this form, we see that the VTPM insists that all communities have an edge density greater than  $\rho^*$ , which very naturally corresponds to the edge density community definition. Communities are weighted by the number of links  $l_A = \frac{1}{2} n_A (n_A - 1)$ .

It is illuminating to contrast the VTPM Hamiltonian of Eq. (17) with the APM Hamiltonian of Eq. (14). They appear identical, with the exception of the APM's inclusion of a scale factor of  $\frac{1}{1-\rho^*}$ . This means that *all past work on the APM applies equally to the VTPM*. In particular, we do not need extensive additional testing on the VTPM in order to show that it achieves the same performance. The APM scale factor of  $\frac{1}{1-\rho^*}$  becomes negative when  $\rho^* > 1$ . In all of our analysis thus far, this would not seem to be a limitation, but when we consider weighted graphs in Sec. X, it will. This is the first advantage of the VTPM over the APM.

A ‘‘clique’’ is a group of nodes all mutually connected (thus,  $\rho = 1$ ). Normally, community detection methods do not break up cliques, because they are as strongly connected as possible. However, if the edges are weighted, there may be certain ‘‘weak’’ edges where it is reasonable to separate communities. In the APM, weighted cliques can not be subdivided, since it only places energy penalties at *missing* edges. The VTPM overcomes this limitation by allowing the least weighted edges to become repulsive repulsive first as  $\rho^*$  is increased. Cliques can

then be subdivided at their weakest point. The VTPM is so named because it is able to ‘‘change the topology’’ of these cliques.

The core advantages of the VTPM over the APM are the ability to break up cliques and handle weighted graphs more naturally. Otherwise, it contains the same information as the APM. Instead of the control parameter  $\gamma = \frac{\rho^*}{1-\rho^*}$ , it uses  $\rho^*$  directly, leading to a much more natural interpretation of the community scale. Because of this, the VTPM provides a compelling community detection algorithm for future use, which will be elaborated on in future sections.

### C. Discussion of Potts models

The APM has been extensively studied and shown to have acceptable performance in community detection across a wide variety of conditions and problems, including common equal-sized and power law distributed graphs [39, 46]. Since we have shown that the APM directly uses the edge density community definition (although unstated explicitly until now), even without additional tests, we have strong support for the edge density community definition. While the VTPM has not been as extensively studied, by comparing Eq. (14) and Eq. (17), we see that the Hamiltonians are the same for unweighted graphs, save a scale factor of  $\frac{1}{1-\rho^*}$ . This means that the VTPM also will be equally powerful in all of the above cases.

### D. Energy changes upon community assignment perturbation

The APM and VTPM are sums over all edges provided they connect nodes in the *same community*. Thus, when we make some change to the community assignments, for example, by combining two communities, the energy change is completely represented by the sum of energies from edges which were just moved into the same community, minus sum of energies from edges which have been removed from the same community. As an example of this, consider adding node  $x$  to community  $B$ , Fig. 1 (b). The entire APM energy remains unchanged except for the  $n_B$  links between  $x$  and the nodes of  $B$ . Thus, the energy change can be represented as

$$\begin{aligned} \Delta E &= \sum_{b \in B} (A_{bx} - \gamma B_{bx}) \\ &= e_{Bx} - \gamma (l_{Bx} - e_{Bx}) \\ &= l_{Bx} \frac{\rho_{Bx} - \rho^*}{1 - \rho^*}. \end{aligned} \quad (19)$$

In the above,  $A_{bx}$  and  $B_{bx}$  correspond to the adjacency and inverse adjacency matrices as defined previously, while other uses of  $B$  within subscripts correspond to

the community  $B$  in Fig. 1. For the VTPM, the energy change upon perturbation is also analogous,

$$\Delta E = l_{Bx} (\rho_{Bx} - \rho^*). \quad (20)$$

The energy changes via perturbation have the same form as for the global energy, with the sum only over the subset of edges created, and the subtraction of only a sum over the subset of edges removed. The local nature of energy makes it fast to compute energy changes under system perturbations. Community detection then becomes a fairly well understood problem of sampling an energy landscape with local interactions, using dynamics of the user's choice.

Using Eq. (19), we can see that a node  $x$  will join a community  $B$  (Fig. 1 (b)) if the node-to-community edge density is  $\rho_{Bx} > \rho^*$ . A node  $e'$  will *leave* a community  $E$  (Fig. 1 (e)) if the node-to-community edge density is  $\rho_{Ee'} < \rho^*$ . We can also show that two communities  $C, C'$  will merge (Fig. 1 (c)) if the inter-community edge density is  $\rho_{CC'} > \rho^*$ . Thus, edge density naturally describes all possible community merges, with  $\rho^*$  being the critical edge density for all possible merges or splits.

The above shows that communities returned by the Potts models satisfy (b) and (c) of the edge density community definition, Sec. II A. Criteria (c) states that community  $B$  will have every node  $\rho_{Bx} > \rho^*$ . If this was not true in a community, energy would be lowered by removing node  $x$  from the community via the inverse of Eqs. (19,20). Criteria (b) states that a community  $B$  will grow as long as  $\rho_B$  stays greater than  $\rho^*$ . This is evidenced by the fact that any node  $x$  with  $\rho_{Bx} > \rho^*$  will have a favorable energy change upon joining  $B$ , growing  $B$  is large as possible as long as all nodes have sufficient node-to-community edge density. Eq. 22 ensures that the resulting community has  $\rho_B > \rho^*$ .

#### IV. MODEL-INDEPENDENT COMMUNITY PROPERTIES

The edge density  $\rho$  is not just an arbitrary variable selected because it is simple and leads to a consistent definition of community. It has many theoretical properties which can be compared to real communities, and helps in the formulation of a consistent community detection framework. In this section, we will derive various properties of  $\rho$  which will prove useful in the exploration of the edge density community definition.

Consider a community  $A$  with  $n_A$  members  $a_i$  (Fig. 2). The edge density within  $A$  is  $\rho_A$ . Each node  $a_i$  has an edge density to the rest of the community  $\rho_{a_i}$ . The first property which we will show is that the edge density of the community is equal to the average edge density of the component nodes to the community,

$$\rho_A = \langle \rho_{Aa_i} \rangle, \quad (21)$$

with the average taken over different community members  $a_i$ . To show this, we apply the edge density Eq. 1

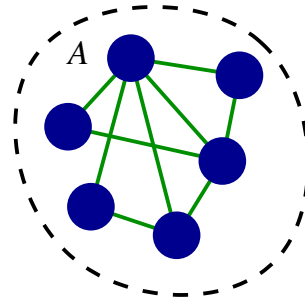


FIG. 2: Illustration of average mean community edge density. Community edge density  $\rho_A \frac{9}{16}$  is equal to the mean of all node edge densities  $\frac{1}{6} (\frac{5}{5} + \frac{2}{5} + \frac{4}{5} + \frac{3}{5} + \frac{2}{5} + \frac{2}{5}) = \langle \rho_{Aa_i} \rangle$ . This, and other similar invariants, are among the properties of edge density.

and evaluate the average in Eq. (21). This leads to

$$\begin{aligned} \langle \rho_{Aa_i} \rangle &= \frac{1}{n_A} \sum_a \frac{e_{Aa}}{l_{Aa}}, \\ &= \frac{e_A}{\frac{1}{2} n_A (n_A - 1)}. \end{aligned} \quad (22)$$

In the above, the number of links for each node is constant at  $l_a = n_A - 1$ , and  $\frac{1}{2} n_A (n_A - 1)$  is the number of links in a community of  $n_A$  nodes.

Next, when a node  $x$  joins a community  $A$  to form community  $A \cup x$ , there is a relationship between the edge density of the combined unit  $\rho_{A \cup x}$  and that of the component edge densities  $\rho_A$  and  $\rho_{Ax}$ ,

$$\begin{aligned} \rho_{A \cup x} &= \frac{e_{A \cup x}}{l_{A \cup x}} = \frac{e_A + e_{Ax}}{l_A + l_{Ax}}, \\ &= \frac{l_A}{l_A + l_{Ax}} \rho_A + \frac{l_{Ax}}{l_A + l_{Ax}} \rho_{Ax}, \end{aligned} \quad (23)$$

which is simply the mean of  $\rho_A$  and  $\rho_{Ax}$  weighted by the respective numbers of links  $l_A$  and  $l_{Ax}$ .

A similar relationship can be shown for two non-overlapping communities  $A$  and  $B$  with initial edge densities  $\rho_A$  and  $\rho_B$  and an inter-community edge density  $\rho_{AB}$ . When two communities merge, the new edge density is the average of the edge density of  $A$ , the edge density of  $B$ , and the inter-community edge density  $\rho_{AB}$ , weighted by the corresponding number of links  $l_A$ ,  $l_B$ , and  $l_{AB}$

$$\rho_{A \cup B} = \frac{l_A \rho_A + l_B \rho_B + l_{AB} \rho_{AB}}{l_A + l_B + l_{AB}}. \quad (24)$$

These properties are useful for considering dynamics of community detection algorithms. For example, for a community  $A$  and a node  $x$ , if we know that  $x$  should join  $A$  ( $\rho_{Ax} > \rho^*$ ), then the final edge density of  $A$  ( $\rho_{A \cup x}$ ) can not decrease below  $\rho^*$ . Furthermore, if we have two communities  $A$  and  $B$  (with  $\rho_A > \rho^*$  and  $\rho_B > \rho^*$ ), if the inter-community edge density  $\rho_{AB} > \rho^*$  (the criteria for community merging), then, after merging, we are guaranteed that the new community  $A \cup B$  must have  $\rho_{A \cup B}$

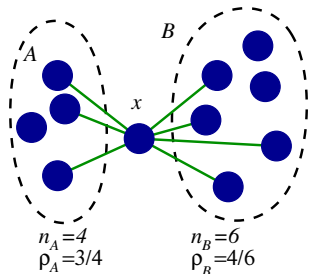


FIG. 3: Balance between placing a node  $x$  into community  $A$  or  $B$ . In this plot,  $x$  has a sufficient edge density to join either community, but when overlapping community assignments are not allowed, we can have  $x$  join both. The text discusses the criteria that edge density models use to assign  $x$  to either  $A$  or  $B$ .

satisfying the edge density condition  $\rho_{A \cup B} > \rho^*$ . These properties serve as a basic check on the sensibility of our community definition.

When  $\rho^* = 1$ , then all communities must be fully connected (only graph cliques are allowed as communities). When  $\rho^* > 1$ , communities can not exist as edge density can not be greater than one. In this case, most CD methods will return “communities” which actually consist of single nodes, since there is never a case that multiple nodes can join together. When  $\rho^* = 0$ , there is no lower bound for community size, and all nodes can collapse into one large community spanning the system, however, this may not happen if the graph consists of disjoint subsets of nodes and the exact dynamics of the CD process does not attempt to join disjoint sets of nodes together.

## V. MODEL-DEPENDENT COMMUNITY PROPERTIES

The discussion of the properties in the previous section makes one critical assumption: when nodes are added to communities, they are previously “unassigned,” or in single-node zero-energy communities. In these cases, there is no energy barrier for removing nodes from the previous community to which they are bound. This is the case when constructing local communities, or when overlapping communities are allowed. When this is not the case, in order to add a node  $b$  to community  $A$ , it must first be removed from some other community, say  $B$ . Since the node  $b$  is in community  $B$ ,  $b$  must have a binding energy to  $B$  that must first be overcome. Any energy released by moving  $b$  to  $A$  must first offset the energy needed to remove  $b$  from  $B$ . In order to determine trade-offs between larger communities and greater edge density, we must use the Hamiltonian from one of our set of models. Towards this end, without loss of generality, we may use the APM.

In order to demonstrate the choices which the edge density models make, we will use a simple thought experiment of one node  $x$  which can either join community

$A$  or  $B$ , as in Fig. 3. As a precondition, we must have  $\rho_{Ax} > \rho^*$  and  $\rho_{Bx} > \rho^*$ , otherwise  $x$  can not join both communities. According to the edge density community definition, with  $\rho_{Ax} > \rho^*$  and  $\rho_{Bx} > \rho^*$ , in isolation, or if overlapping community assignments were allowed, it would be allowable for  $x$  to join either community, and this would be the preferred energy-minimizing move. When overlaps are not allowed,  $x$  must choose one of  $A$  or  $B$  to join.

A similar situation occurs when node  $b$ , part of community  $B$ , has a sufficient edge density to also join  $A$ . The energy of addition to  $A$  must at least compensate for the energy of removal of  $b$  from  $B$ . We imagine this in two parts: first, the removal from  $B$ , and second, the choice between addition to  $A$  or  $B$ , allowing us to consider only the  $A, B, x$  situation of the previous paragraph without loss of generalization.

When using the VTPM, the node  $x$  will choose to join the community which most minimizes the energy. It will join  $A$  when  $E_{Ax} < E_{Bx}$ , which can be rearranged to

$$n_A [\rho_{Ax} - \rho^*] > n_B [\rho_{Bx} - \rho^*]. \quad (25)$$

We see that  $x$  will join the community  $A$  or  $B$  to which it has the largest excess edge density  $\rho_{Cx} - \rho^*$ , weighted by the community size  $n_A$  or  $n_B$ . We note the following: (a) we assume  $\rho^* < 1$ . The cases where  $\rho \geq 1$  are discussed above. (b) we assume  $\rho_{Ax} > \rho^*$  and  $\rho_{Bx} > \rho^*$ . If both are less than  $\rho^*$ ,  $x$  can join neither community, if one is less than  $\rho^*$ , we see the node will join the other community (c) If  $\rho^* = 0$ , then  $x$  will join the community of greater size. (d) If  $\rho_{Ax} = \rho_{Bx}$ ,  $x$  will join the community of greater size. (e) if  $n_A = n_B$ , according to Eq. (25),  $x$  will join the community to which it has greater  $\rho$ .

We see that these results support the idea that a node, when faced with other communities of equal sizes, will join the community to which it shares the greatest edge density, however, there is also a competing preference towards smaller, more dense, communities.

It deserves emphasis that the results from this section are derived for one particular instance of the edge density community definition, the one derived from the VTPM. For unweighted graphs, this model will give equivalent results to the APM. The APM has been shown to be an effective community detection method in a wide variety of situations [38, 39, 46].

## VI. SIMPLE EDGE DENSITY COMMUNITY DETECTION ALGORITHMS

The purpose of this paper is not to discuss specific edge density community detection algorithms, instead, we focus on the *ground-state* properties of this community definition. There are various published algorithms which can be used directly with edge densities. Previous work from our group used a global algorithm, beginning with every node in a different community and merging communities

until some energy minimum is reached[38, 39, 49, 50]. Alternatively, there are various local methods, which build up a single community around single nodes[51–53].

Unlike other methods, there is no heuristic for determining the proper  $\rho^*$ . Instead, we use a multi-replica inference method where independent “replicas” are solved at the same value of  $\rho^*$ , and their similarity is compared. If, for a given value of  $\rho^*$ , the independent replicas minimize to give similar community structures, this is considered to be a “good” value of  $\rho^*$ . This has proven to be a reliable and robust method for community detection. For addition information, see Sec. A 4.

Further information and considerations about these methods is found in Appendix A.

## VII. EDGE DENSITIES IN REAL NETWORKS

Our edge density definition assumes that  $\rho^*$  is a useful resolution parameter, which can select for larger or smaller communities. We have operated on an intuition that a larger  $\rho^*$  selects for a smaller, more densely connected communities, while a smaller  $\rho^*$  selects larger, less densely connected communities. In this section, we will directly consider this assumption. Recently, Yang and Leskovec (YL) have taken a variety of real networks, mainly social networks, and rigorously studied their properties with respect to size, overlap regions, and other parameters[40]. They find that the number of edges within a community tends to grow with a power in the range (1, 2), with observed values of 1.1 and 1.5. For some exponent value  $\nu$ , it is thus found

$$e \propto n^\nu. \quad (26)$$

However, maximal number of edges ( $l$  in our nomenclature) grows as

$$l = \frac{1}{2}n(n-1) \propto n^2, \quad (27)$$

thus we find a scaling relation of edge density of

$$\rho = \frac{e}{l} \propto \frac{n^\nu}{n^2} \propto n^{\nu-2}. \quad (28)$$

As long as  $\nu \in (1, 2)$ , we find  $\rho$  decreases as  $n$  increases. For example, YL observed social networks to have an exponent value of  $\nu \approx 1.5$ , giving us

$$\rho \propto n^{-.5}. \quad (29)$$

As we see, this validates one of the central tenets of the edge density community definition: as communities grow larger, the edge density tends to decrease. By specifying a  $\rho^*$ , we implicitly specify a size scale of community which we will then detect. Another way to view this is from the standpoint of an agglomerative community detection algorithm. Starting from a dense core, as each additional node is added to a given community, the community edge

density on average decreases with each additional node, lowering the edge density. As we keep adding nodes to the community, eventually, the community will grow so large that adding extra nodes will decrease  $\rho$  below  $\rho^*$ .

## VIII. OVERLAPPING COMMUNITIES

Many networks have community structure which can most naturally be described as *overlapping*. In this viewpoint, there are certain nodes which can be reasonably included in multiple groups. Perhaps the most standard example of this situation is social networks: any one person will be involved in groups corresponding to work, family, hobbies, etc. The overlaps can consist of single nodes or larger subsets. Not all community detection methods can be extended to handle overlapping nodes. For example, the Newman betweenness algorithm progressively cuts edges until modularity maximization states that final communities are found [13]. Because each cut is final, there is no ability to create overlapping communities. Different methods, such as clique percolation [7], attempt to detect overlapping community structure. There are a variety of local community definitions, including the community-centric Potts model formulations of Eq. (8), can detect overlapping communities by virtue of *independently* detecting each community[51].

The work of YL also looked at the characteristic of overlapping regions of communities[40]. According to the behavior seen by YL, regions of overlap between communities have edge density contributions from both communities[40, 54, 55]. Thus, these overlap regions have a greater density than the individual communities. It had previously been assumed that these regions of overlapping communities had a smaller edge density than either of the non-overlapping regions, and past methods of community detection make the opposite assumption, and thus not suitable for community detection with the observed behavior [7, 56, 57]. We can show directly that the edge density community definition properly handles this case.

Let us look at a diagram of two overlapping communities  $A$  and  $B$ , embedded in a universe of nodes (Fig 4, upper). We denote the universe of nodes  $U$ , the two communities  $A$  and  $B$ , the region of community  $A$  excluding  $B$  as  $A - B$  and vice versa, the overlap region  $A \cap B$ , and the universe of nodes excluding either community,  $U - A - B$ . Fig. 4 is a schematic of this situation. Communities  $A$  and  $B$  both have internal edge densities of .5. The overlapping region  $A \cap B$  has an edge density of .75. The edge density between  $A - B$  and  $A \cap B$  is .5, and vice versa for  $B$  and  $A$ .

With  $\rho^* = .75$ , only the overlapping region  $A \cap B$  will be detected, with  $\rho^* = .5$ , communities will expand to cover the region  $A$  or the region  $B$ , but not  $A \cup B$ . The reason for this is that, if we have currently detected the community  $A$ , any one node  $x$  in  $B - A$  will have a  $p = .5$  edge density to  $A \cap B$ , but only  $p = .5$  edge density

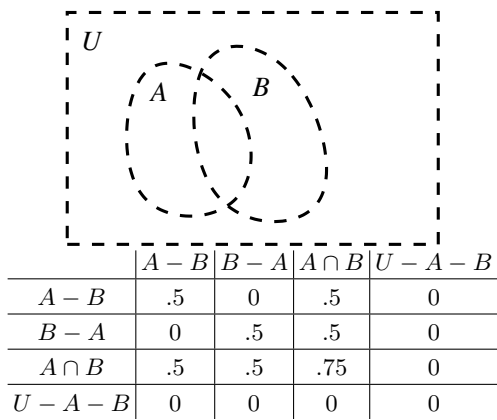


FIG. 4: Schematic of two communities  $A$  and  $B$  with  $p_A = p_B = .5$ , and their overlap edge densities. This illustrates the affiliation graph model edge densities between each of the distinct regions of the figures, with a “dense overlap” in the  $A \cap B$  region, as determined by YL [40]. According to YL, currently existing community definition models can not detect these communities. The table indicates the probability for an edge being present between any two regions of the plot: the “-” operator indicates set difference,  $A - B$  indicates the region of  $A$  excluding  $B$ .

to  $A - B$ , thus the average connection probability to the entire set  $A$  is  $p_{Ax} \frac{.05n_{A-B} + .5n_{A \cap B}}{n_A} < .5$ , thus,  $p_{Ax} < \rho^* = .5$ . This is the desired behavior. The same will be true of a node  $y$  in  $A - B$  attempting to join community  $B$ . Thus, by applying the edge density community definition, we can get exactly the desired behavior: for  $\rho^* = .5$ , we detect  $A$  and  $B$ , while for  $\rho^* = .75$ , we detect  $A \cap B$ .

## IX. THE AFFILIATION GRAPH MODEL

In order to model the properties they observed, YL described the “Affiliation Graph Model” (AGM)[40]. This model is similar to stochastic block models in that edges are drawn in only based on the community memberships of the two nodes. However, nodes are allowed to belong to multiple communities, and the communities are not restricted to being disjoint. This can be interpreted as a bipartite graph from “people” to shared “affiliations”. In the AGM itself, the affiliations are not present, and instead each shared affiliation incorporates chance of shared edge between “people” (nodes in the graph). A similar concept of affiliations grouping has been considered before in a sociological and network context[55, 58], and such work has hinted that under certain generation processes, such models could produce power-law distribution of node degrees[40]. Because this benchmark model incorporates dense overlap, YL claim that current community detection methods are not able to successfully detect communities in this type of graph.

The basic idea behind AGMs is that communities (“affiliations”) are chosen from a universe of nodes. These could be non-overlapping and spanning the uni-

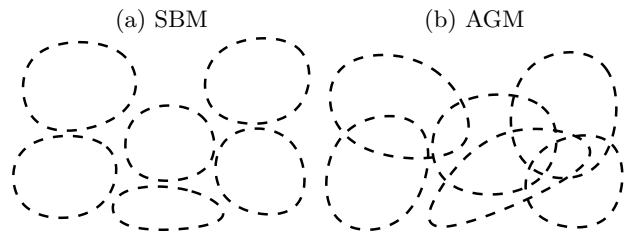


FIG. 5: Schematic of stochastic block models (SBM) vs affiliation graph model (AGM) graphs. (a) The SBM graphs are non-overlapping, while (b) the AGM graphs allow overlaps. Note that in our specific instances of AGM graphs, every node is in at least one community.

verse (yielding a *planted  $l$ -partition*, or Stochastic Block Model), or any assortment of hierarchical, overlapping, subset-containing, or other arrangements. Then, we add an edge with probability  $p$  for *each* shared affiliation. Since there can be multiple shared communities per node, we allow each shared affiliation a chance to produce an edge. This gives us an ultimate edge probability between nodes  $x$  and  $y$  of

$$p_{xy} = 1 - \prod_C (1 - p_C) \quad (30)$$

where the product is over all communities  $C$  which contains both nodes  $x$  and  $y$ . This is the complement of the probability that none of the shared affiliations produce a community.

The instance of AGM networks we study here is constructed as such: A universe of  $N$  nodes is taken. We take  $q$  communities of  $n$  nodes each, with  $nq \geq N$ , in two steps: first, we initialize the communities with non-overlapping communities of  $N/q \leq n$  nodes. Then, for each community, we add additional nodes necessary to make  $n$  nodes per community by randomly choosing from all other nodes. There are no restrictions to the maximum number of communities to which a node can belong. The edge probability between any two nodes is given by Eq. (30). Our particular AGM graphs can be identified by the parameters  $(q, n, p)$ . The AGM benchmark graphs differ from stochastic block model graphs by allowing overlaps, Fig. 5.

Further, we may produce *multi-layer* benchmark graphs. It is traditional to produce hierarchical graphs for consideration, where small communities are contained within single large communities. To create our multi-layer graphs, we create AGM graphs *independently* over the same universe of nodes, and then merge the set of edges. There is no requirement that each small community be contained within a single large community, and in fact, for each community, each small community is likely to overlap with *every* large community. The amount of overlap present here is unparalleled in the existing literature. Fig. 6 illustrates the difference between hierarchical and multi-layer community assignments. To produce multi-layer AGMs, we take two AGMs inde-

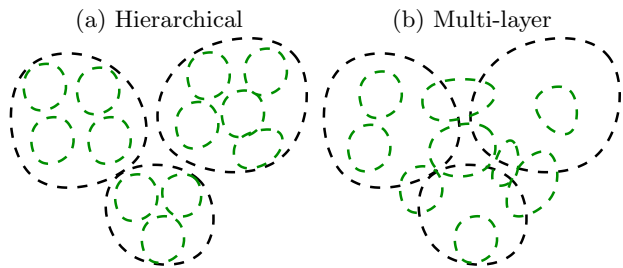


FIG. 6: Schematic of hierarchical vs multi-layer. (a) The hierarchical graphs have small communities (smaller circles, green) contained entirely within large communities. (b) The multi-layer graphs have small communities which are allowed to span multiple large communities. In our specific instances of AGM graphs, every node is in at least one community, and small communities are assigned *completely* independently of large communities, allowing extremely high degrees of mixing between small and large communities. There have been no proposals of this type of multi-layer community detection in the literature, but we will demonstrate our methods detecting these communities properly.

pendently from the universe of nodes and overlay edges. Edge probabilities are still calculated via Eq. (30), but now the sum over communities  $C$  contains multiple layers of communities. We denote our multi-layer AGMs via the nomenclature  $((q_1, n_1, p_1), (q_2, n_2, p_2))$ . Our final graphs are thus a combination of the overlaps of Fig. 5 and multi-layer character of Fig. 6.

We now examine actual results from application of the absolute Potts model and variable topology Potts model to our overlapping community benchmarks using the multi-replica inference framework of Sec. A 4. We use the F-score measures of Appendix C to judge the performance of our algorithms. We study both inter-replica  $F_1^{IR}$ , which is used to identify the correct  $\rho^*$ , and  $F_1^0$ , a measure of how well we detected the planted communities. According to the canonical multiresolution algorithm, extrema of uniformity between replicas ( $F_1^{IR}$ ) indicate  $\rho^*$  (or  $\gamma$ ) values likely to be significant.  $F_1^0$  indicates how well we detect the planted communities. In practice, we want a maximum of  $F_1^{IR}$  to correspond to the maximum of  $F_1^0$ . When both of these measures to peak at the same value of  $\rho^*$  to indicate that we can recover the planted states and that we would be able to infer the correct value of  $\rho^*$  if the planted states were not known *a priori*.

Fig. 7 shows results for single-layer AGM graphs. We see that we can perfectly recover communities for both situations, and are able to infer the correct value of  $\rho^*$  (or APM  $\gamma$ ) without *a priori* knowledge. We see that we are not only able to detect the planted communities (planted  $F_1 = 1$ ), but to know where that would be (inter-replica  $F_1 = 1$ ). Fig. 8 shows results from application to multi-layer AGM graphs. We see accuracy comparable to single-layer graphs, with slightly less well defined peaks. It should be noted, we can not solve this

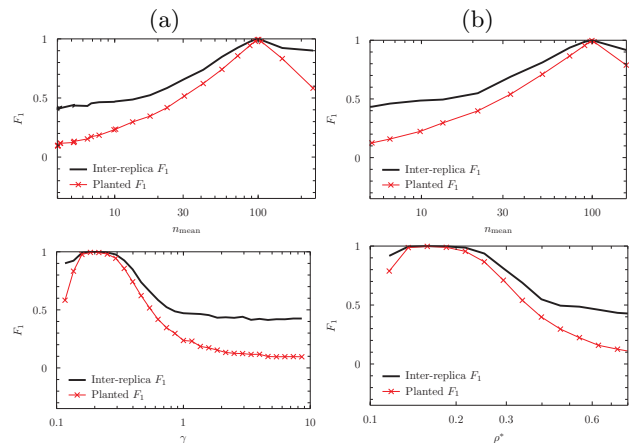


FIG. 7: Community detection results on single-layer AGM graph with parameters number of communities  $q = 20$ , number of nodes per community  $n = 100$ , and edge probability  $p = .25$  in a total universe of  $N = 1000$  nodes, showing perfect community detection.  $F_1^0$  indicates our ability to detect the known community structure; a value of unity indicates perfect community detection.  $F_1^{IR}$  indicates our ability to locate the correct resolutions (value of  $\rho^*$ ) without *a priori* information about community sizes. When both measures becoming unity at the same  $\rho^*$  value, our methods can both infer the correct resolutions and achieves perfect detection at that resolution. Similar results are achievable with a wide range of AGM parameters, demonstrating robustness of the methods. Upper plots show community detection with respect to  $n_{\text{mean}}$ , showing that the methods do indeed detect the correct community size  $n = 100$ . The column (a) uses the absolute Potts model, and the column (b) uses the variable topology Potts models. The lower plots show the role of the respective scale parameter  $\gamma$  for the APM and  $\rho^*$  for the VTPM.

for arbitrary parameters. The  $(q, n, p)$  of the two layers are hand-chosen to give good results by adjust the probabilities of large and small communities. Because of this, the methods here would not necessarily be useful for real graphs. We choose this example to demonstrate the power and limitations of the method. It is unlikely that real graphs would be as complex to solve as the multi-layer fully independent random case.

In a future work, we will systematically apply edge density methods to a wider variety of AGMs, demonstrating the usefulness of edge density methods. The models we will consider will include various combinations of power law community sizes, different forms of hierarchy, communities within communities, homeless nodes, and more. In addition, we will provide theory information regarding the limits of edge density methods in the face of large amounts of dense overlap.

## X. WEIGHTED GRAPHS

One area of modern community detection research is the subject of weighted graphs. In weighted graphs, not

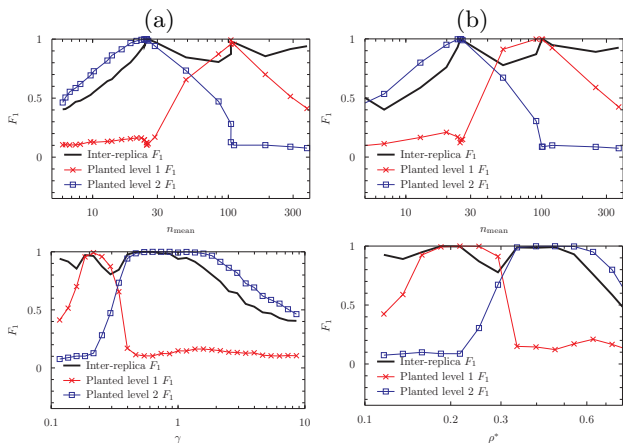


FIG. 8: Community detection results on multi-layer AGM graphs.

Multi-layer AGM graphs with parameters (a) ( $(q_1 = 16, n_1 = 100, p_1 = .3), (q_2 = 64, n_2 = 25, p_2 = .75)$ ) and (b) ( $(q_1 = 16, n_1 = 100, p_1 = .35), (q_2 = 64, n_2 = 25, p_2 = .75)$ ). Both inter-replica and known detection measures are plotted as in Fig. 7. Note that these parameters are “cherry-picked” to give good results; successful community detection is not possible for arbitrary parameters. At arbitrary parameters, one layer is perfectly detectable and one layer is noticeable but without perfect detection. Upper/lower rows and left/right columns maintain the same interpretation as in Fig.7

every edge has equal importance. Any modern community detection method should be able to handle weighted graphs. A high weight will indicate an edge which plays a major role in the graph, while a low weight indicates an edge which does not significantly affect the graph. An unweighted graph can be considered a weighted graph of edges of weight one, so by convention, a weight of zero corresponds to an edge which is not present, and a weight of one corresponds to an unweighted edge.

In order to adapt edge density to weighted graphs, we make a simple substitution. We consider the number of edges to be the sum of weights of all edges  $i$ ,

$$e = \sum_i w_i \quad (31)$$

with the sum taken over all edges. Thus, the edge density for any grouping of nodes  $X$  is

$$\rho_X = \sum_{i \in X} \frac{w_i}{l_X}. \quad (32)$$

The grouping  $X$  can be that of any community  $A$ , a pair of communities  $AB$ , or any of the other situations depicted in Fig. 1. As to be expected for any reasonable extension of its counterpart of the unweighted graphs, we note that, indeed, for unweighted graphs Eq. (32) reduces to the same definition appearing in Eq. (1). Furthermore, edges can be weighted greater than one for very important edges. Adversarial edges (edges which favor being in different communities) can be weighted less

than zero. All of our analysis in the previous sections remains valid *mutatis mutandis*, with the caveat that  $\rho$  is no longer limited to the range  $[0, 1]$ . The edge density can exceed unity when there are many edges with weight greater than one, or less than zero if there are enough adversarial edges. Furthermore, we maintain a property of linearity of edge densities. If linearity is not desired, a power (or other mapping function) could be applied to edge densities before summing to get the “number of edges” stand-in.

The APM Hamiltonian, Eq. (8), can handle weighted graphs, with  $A_{aa'}$  being a matrix of edge weights for present edges and  $B_{aa'} = 1$  if there is no edge. There are two caveats. First, the APM model uses the number of missing edges, for which we use  $l - e$  in Eq. (9) (the maximal number of possible edges, minus the number of actual edges). However, when  $e = \sum w_i$ , this is no longer necessarily true:  $e$  no longer is identical with the number of existing edges. Thus, Eq. (14) no longer corresponds to Eqs. (7, 8) Second, in our final density formulation of the APM Hamiltonian (Eq. 14), there is a factor of  $\frac{1}{1-\rho^*}$ . This becomes zero or negative when  $\rho^* \geq 1$ , thus rendering our derivations invalid.

The VTPM avoids both of these limitations, and allows a natural extension to weighted graphs with no discontinuity for  $\rho < 0$  or  $\rho > 1$ . We reiterate that as we have shown that the APM and VTPM are identical for unweighted graphs, we know, even without dedicated experimentation, that the VTPM is a successful community detection method for a broader class of graphs.

## XI. EXTENSIONS

*Multigraphs* are graphs that allow more than one edge to be between any pair of nodes. As we sum over all edges, multigraphs can be very naturally included in the summation over edges. However, note that under this formulation, a multigraph is seen as equivalent to a weighted graph, with each edge having a weight equal to the sum of the weights of the other edges. If this procedure loses essential information about the graph, a different method will be needed. Perhaps multiple edges could be combined into one with a different weighting function, however, without a rigorous analysis of the most important aspects of multigraphs, we can only speculate. For now, all we do is point out that edge density is not incompatible with the concept of multigraphs.

If our graphs have multiple types of edges, or multiple distinct forms of weight per edge  $w_0, w_1, \dots$  generalized to a vector  $\hat{\mathbf{w}}$ , we can generalize the total edge weight as a weighted average  $w = \hat{\mathbf{w}} \cdot \hat{\mathbf{u}}$ , with  $\hat{\mathbf{u}}$  being a unit vector weighting the different individual weight contributions. This allows us to use a different combination of component weights depending on our intended community detection goals.

The methods presented in this paper use only edges, and not higher order correlations such as triangles (3-

cliques). In order to use e.g. triangles, we would define a “triangle density” as

$$\rho_C^t = \frac{t_C}{\frac{1}{6}n_C(n_C - 1)(n_C - 2)} \quad (33)$$

with  $t_C$  being the number of triangles in community  $C$ ,  $n_C$  being the number of nodes in community  $CC$ , and the denominator being the maximal possible number of triangles in community  $C$ . This could be extended to a number of other higher-order correlations of any structural motif rather trivially. Many real networks have been shown to contain non-trivial patterns in these higher order correlations, which are for the most part not presently considered in community detection methods[59].

## XII. DISCUSSION

Despite edge density well describing many benchmarks and real graphs in an effective manner, our definitions and protocols have certain limitations. While these limitations exist, past use of edge density methods has shown they are not barriers for most important problems. The edge density community definition is *simple*. Thus, we expect the edge density community definition to be general and easily extendable.

For large sparse networks, the total number of edges is proportional to the number of nodes ( $e \propto cn$ ,  $c = O(1)$ ), while the number of possible edges is  $l \propto p\frac{1}{2}n(n-1)$ . The edge densities are driven to zero exists as the number of nodes per community  $n$  increases,

$$\rho \propto \frac{e}{l} \propto \frac{cn}{p\frac{1}{2}n(n-1)} \propto \frac{c}{pn} \rightarrow 0. \quad (34)$$

When all edge densities become small, it become progressively more difficult for the parameter  $\rho^*$  to distinguish communities. This general problem is discussed in more general terms in a companion work [60]. Overall and inter-community edge density decreases with  $N$  (total number of nodes), while intra-community edge density decreases with  $n$ , the number of nodes per community. However, in the case of somewhat fixed-sized communities, the inter-community edge density is driven low much faster than intra-community edge density, allowing  $\rho$  to still be successfully used to distinguish the communities. The success of edge density community definition will depend on the precise graph and “ground-truth” community characteristics, and can be studied over various classes of graphs.

Studies of real networks have shown a power law distribution of community sizes[7, 61, 62]. A variation of community size does not affect the edge density community definition, as long as the community has a uniform  $p$  of each edge existing, the edge density community definition will be able to properly detect its communities.

Studies have also shown that real networks have power-law distributions of node degrees[59, 63–65]. If, upon

further analysis, this power law degree distribution corresponds to a power law distribution of *internal* degrees (number of edges connecting to other nodes inside a community), then the distribution of node ( $a$ ) to community ( $A$ ) densities  $\rho_{Aa} = e_{Aa}/(n_A - 1)$  will then be power law distributed as well. The edge density community definition can still be relevant to these graphs. In these cases,  $\rho^*$  will determine the edge density for the lowest-degree nodes of the community. The high-degree nodes will still be included as part of the community to which they have the greatest connecting edge density. If a high-degree node has many of its edges spread out among other communities, it will not be misclassified as long as its node-to-correct-community edge density is greater than  $\rho^*$  and it shares the greatest edge density with the correct community. The work of Lattanzi and Sivakuma [66] provides another possibility which will be investigated in a future work. Using a model similar to AGMs, they have shown a natural appearance of power law behavior in affiliation graphs. If this holds for AGMs, then power law node degrees may be consistent with constant internal densities - rendering our current work indeed relevant.

According to the simple definitions listed here, *every* node must have an edge density of greater than  $\rho^*$  to its community. This appears to be a fairly heavy restriction: if there is a node with less than  $\rho^*$  edge density to *any* other community, it will be forever alone. One method of working around this would be to then allow isolated nodes to join whatever community they have the greatest edge density connection with. Alternative schemes could be developed, where only the average community edge density must be greater than  $\rho^*$ , and certain individual nodes can have an edge density of less than  $\rho^*$ . Regardless, internal edge density is only capable of detecting assortative communities, where nodes are connected to similar nodes.

In reality, no single community definition is expected to work across all classes of graphs. Edge densities may describe graphs arising from a certain generation process (such as shared affiliation social networks), information flows may describe data-centric networks, and other methods may describe scientific citation networks, among many possibilities. Certain community definitions should not be studied at the exclusion of others, and it is important to understand all community definitions to know the realm of their applicability. Furthermore, rigorously understanding the resulting communities from a variety of community detection algorithms provides a tantalizing inverse-community detection possibility. Suppose we had a graph which an unknown complex structure, but we *did* know ground-truth communities. By applying community detections algorithms to this graph, and comparing the returned communities to the planted communities, we may learn something about the graph generation process itself.

### XIII. AVOIDING OVER-OPTIMIZATION

As stated in Sec. IIB, the edge density variable  $\rho$  is directly analogous to the probability  $p$  used to generate many common benchmarks. Since our detection method exactly matches the creation processes of common benchmark graphs, it is easy to understand why we achieve such accurate detection. Our definition will be useful for the cases where real graphs are generated in an analogous manner. A current topic of research is the *processes* which generate various real-world networks; for example, processes have been proposed giving rise to power law degree distributions, and also with constant edge probability, as in AGMs. Once more is known about these processes, we can better understand what community definitions are optimal. In addition, there is no reason to believe that one community definition will be optimal in all types of graphs, and we must have many available techniques in our toolbox to be able to respond to whatever problems may occur.

Nevertheless, many current benchmark graphs *are* generated using edge densities, and can be described as such. Our companion work expands on this, and uses edge density - the lowest common denominator of many methods, to learn about the structural source of community detection limits in stochastic block model graphs. Furthermore, due to the highly symmetric nature of these equal-sized stochastic block model graphs, our edge density results generalize to almost all community detection methods.

### XIV. CONCLUSIONS

Edge density community detection methods have been used before, but despite this fact, the underlying theory of such methods have not been explicitly defined and fully explored. This work fills this gap, and in the process formally expands the edge density community definition to include important new classes of graphs, such as weighted graphs, and the possibility for overlapping communities. One of the most important features of our edge density community definition is that it *simple*. One equation,  $\rho = e/l$  (Eq. (1)), is all that is needed to express the core concept, yet our definitions and methods apply within communities, between communities, and for specific nodes. This simplicity is directly linked to the generality of the definition.

To make our formulation concrete, we first discussed an existing edge density community definition, the absolute Potts model. Methods based on Potts models have historically proven to be very accurate, but have shown limitations for weighted graphs. To work around this limitation, we proposed a new edge density model, the variable topology Potts model, and shown its equivalence to the absolute Potts model for unweighted graphs. This generalization points the way for community detection in all major types of graphs. It is worth emphasizing that

our edge density is a *local* community definition, where nodes and communities are only affected by their nearest neighbors. This means our algorithm can be easily scaled to large data sets, where only a small portion of the graph is discoverable.

The core of this work involved developing criteria which must be satisfied for any community assignment to be optimal. The criteria are developed with respect to various changes in community structure (community merging, addition of a node to a community, etc.) being energetically favorable. This is an important part of the evaluation of any community definition or algorithm since it provides intuition as to how the algorithms apply to real world graphs. Furthermore, by developing a set of criteria for various community characteristics, one can check that no unrealistic properties emerge. A chief example of such an unrealistic property, and an example of the application of this technique, was Fortunato and Barthélemy's investigation of a community merge criteria within the modularity community definition in order to find that there was a resolution limit[17].

We have applied our edge density methods to the AGM, a recently proposed benchmark graph model[40]. The creators of this benchmark model claim that no currently existing method can solve it, though it is likely that there exist methods other than edge density which also can. We have solved it exactly, and demonstrated why we are able to do so. Our analysis of the AGM hints at the underlying reason for the accuracy of the edge density community definition. We postulate that the reason the edge density community definition performs so well on benchmark graphs is related to the fact that many benchmark graphs are created with an edge probability  $p$  as the independent variable, to which our  $\rho^*$  is analogous. Nevertheless, edge density methods have proven to be valuable when applied to real world networks[47, 50] and the latest standard benchmark graphs (LFR, AGM)[40, 46, 57]. This provides evidence that edge densities, and the properties derived subsequently, *do* in fact reflect characteristics of important real world networks.

### Acknowledgments

We would like to thank Santo Fortunato for careful reading and comments on this manuscript. We would like to thank Dandan Hu for useful discussions. RKD would like to thank the John and Fannie Hertz Foundation for research support via a Hertz Foundation Graduate Fellowship. The work at Washington University in St. Louis has been supported by the National Science Foundation under NSF Grant DMR-1106293. ZN also thanks the Aspen Center for Physics and the NSF Grant #1066293 for hospitality.

## Appendix A: Simple edge density community detection algorithms

In the past few sections, we have outlined the ingredients necessary for a community definition based on edge density. We will now outline several simple procedures for applying this definition to an algorithm. These dynamical procedures follow the precedent set by existing literature, and our ability to use our definition, coupled with multiple forms of dynamics, illustrates the separation between community definitions and dynamics of community partitioning.

### 1. Global method of Ronhovde, Hu, and Nussinov (RHN)

This method takes an entire graph, and partitions it together, resulting in a single community assignment for every node [38, 39, 49, 50]. RHN use a global  $\rho^*$  (in the form of absolute Potts model  $\gamma$ ) and demonstrate an adaption to overlapping nodes.

In the RHN approach, we assign every node to a unique community consisting of a single node as there are the same number of initial communities as there are nodes. Then, we make repeated passes of the following changes in community assignments until we reach a point of local stability: one in which none of the following moves will lower energy any further. More explicitly, the moves are:

- *Local shifts.* Choose one node, and change the community assignment of the node to another already-existing community. Accept if the change lowers the energy. If the previous community only consisted of one node, that community vanishes and our number of communities  $q$  shrinks by one.
- *New communities.* Choose one node in a community of more than one node, and attempt to move it into a completely new community (which will then have only one node in it). Accept if the change lowers the energy. This increases the number of existing communities by one.
- *Merges.* Attempt to merge two existing communities. Accept if the change lowers the energy. This move contracts the number of communities by one.

The entire program outline above is a *steepest-descent* algorithm. In order to get over energy barriers, we perform  $t$  independent trials with different random seeds (for either in initial community assignments, or orders of traversing nodes and communities in trials) as a means of gaining improved sampling. Typically, on the order of 5 trials are needed, and this is found to be much more efficient of computer resources than simulated annealing-like algorithms[38, 39, 49, 50].

RHN also created an extension of this approach to overlapping communities[47]. After performing the above

steepest descent non-overlapping algorithm, they take the following until they achieve a locally stable configuration:

- *Overlap expansion.* For each community, attempt to add each node not currently in that community. Do not remove the node from the previous community. The number of communities stays constant, but one community gains an extra node. Accept any additions which lower energy.
- *Overlap contraction.* For each community and for each node in that community which was *not* among the original nodes pre-expansion, attempt to remove that node from the community. Accept any removals which lower energy.

This algorithm has been shown to have exceptionally good performance and efficiency. A disadvantage of the original method is that it uses a global  $\rho^*$ ; more recently Ronhovde and Nussinov extended this approach to inferring local structure [67].

### 2. Local algorithm of Lancichinetti, Fortunato, and Kertész (LFK)

In 2008, LFK developed a local fitness function and corresponding dynamics for local community detection algorithms [51–53]. This function shares some similarity with edge density, although is distinct in using external links as part of the measure of local fitness. Their dynamics can be easily adopted to our Potts models for edge density.

For this method, we choose a starting node from which to base our community designations. We then loop the following steps:

- For each community, take the set of all nodes adjacent to, but not within, the community. Calculate the change in community fitness if each node were to be added to the community. Add only the node which increases the fitness function by the most. Repeat until no further additions can increase the fitness.
- For each community, calculate the change in fitness if each node individually were to be removed. If any node would increase fitness by its removal, remove the one node which most increases fitness. Repeat until no further nodes can increase fitness by their removal.
- Once a locally stable community is found, repeat the procedure starting from another node which has not yet been assigned to any community.

This procedure allows overlapping communities to be found, and allows a locally tunable  $\rho^*$ , as opposed to a global  $\rho^*$ . This method has not been applied to our edge

density community definition, but can easily be via local optimization of Eq. (14). This algorithm provides a method of community detection when only a small portion of the graph is visible.

### 3. Advanced methods

Methods such as simulated annealing or heat bath algorithms are extensions to the above methods [22, 49]. As the edge density community definition is based on a Hamiltonian and not a set of dynamic steps, we have the freedom to choose any dynamical steps we may like to minimize energies. Energy optimization has been extensively studied in the physics literature, and there are many lessons which can be taken from spin glasses, molecular dynamics, and other fields.

It would be useful to study the ability of various methods to overcome local energy barriers. For example, RHN noticed that community merge moves were important in order to surmount local barriers[68]. Without these, single-node community shifts were not able to effectively lower energies. There are subtle differences between the order of additions and removals of the RHN and the LFK methods, which could have impact on the performances of the minimizations. These methods will not be discussed further here.

### 4. Multi-replica inference

In order to use the methods outlined above, we must know  $\rho^*$  before we begin our detection process. Since this, in general, can not be known in advance, we need to infer  $\rho^*$  via some technique. There is an established procedure for this *multi-resolution analysis* in the literature[39].

To do this, we *scan* across a range of values and perform multiple community detections (“ $r$  replicas”) at each  $\rho^*$ . We infer that if the results from community detections at a given  $\rho^*$  are very similar, we have good community detection. This is equivalent to saying that at good values of  $\rho^*$ , we have one dominant community assignment that is uniformly detected. Past work has shown this to be a very good procedure [38, 39, 69].

There are various measures of inter-replica similarity, most based on the concepts of information theory[70–72]. Various proposed choices include the variance of information ( $VI$ ) [38, 73, 74], normalized mutual information ( $I_N$ )[38, 75], and a generalized normalized mutual information capable of handling overlaps ( $N$ ) [51]. In this work, we will use a version of the F-score,  $F_1$  generalized to handle partitions (see Appendix C) [50, 53]. The unifying characteristic of these measures is that they take two complete community assignments and output a number which indicates the similarity of the partitions. Most measures, including the F-score, are normalized as follows: a value of unity indicates perfect agreement in par-

titions, while a value of zero indicates completely decorrelated community assignments.

Our F-score development extends the concept of comparing two partitions of the system to overlapping nodes, similar to, but conceptually simpler than, the developments of Lancichinetti *et. al.*[51]. Our derivation provides more insight into the actual performance of the community detection algorithm. Full details are located in Appendix C. There, we derive a modification of  $F_1$  for comparing entire partitions (instead of single communities) to each other, which we denote  $F_1^R$ .  $F_1^R$  has the following interpretation: a value of unity indicates perfect agreement between community assignments, and a value approaching zero indicates perfect decorrelation of community structure.

These similarity measures ( $VI$ ,  $I_N$ ,  $F_1^R$ , etc.) are also used for testing the outcomes of community detection experiments. If we know the correct community assignments (community assignment  $R_0$ ), we expect the similarity between the detected and correct communities to be unity when averaged across the detected configurations  $R_1, R_2, \dots, R_r$ :

$$S^0 = \frac{1}{r} \sum_{i=1}^r S(R_0, R_i) \quad (\text{A1})$$

using similarity measure  $S$ . To compute the inter-replica symmetry, we use

$$S^{IR} = \frac{1}{r(r-1)} \sum_{i=1}^r \sum_{j \neq i}^r S(R_i, R_j). \quad (\text{A2})$$

Thus we can state our general criteria for a useful multi-resolution algorithm: as a function of  $\rho^*$ , we must have a maximum of  $S^{IR}$  at the same locations as  $S^0$  unity, in order to have both *accurate community detection* and *the ability to infer correct  $\rho^*$  with no prior information*.

### Appendix B: Why do current methods not properly handle dense overlaps?

One of the claims of YL is that current community detection methods do not properly handle dense overlaps as in Fig. 4 [40]. In this section, we will explain why that is for certain popular methods. For our thought experiment, consider two communities  $A$  and  $B$ , with a dense overlap as shown in that figure.

#### 1. Clique percolation

In clique percolation, a  $n$ -clique (set of  $n$  nodes all mutually connected) is located within a graph[7]. Then, all cliques which overlap  $n - 1$  nodes of the first clique are identified. This process continues, and a community is defined as set of all nodes reachable by this percolation process. For both communities  $A$  and  $B$ , the percolating

clique will enter the overlap and detect these nodes. Once that happens, the percolating clique can “jump” to the other community, and they will merge together.

## 2. Betweenness

When using betweenness to detect communities, shortest paths (along graph edges) are drawn between *all* pairs of nodes[13]. The edges with the most shortest paths falling through them are considered the boundary between communities, and are virtually removed, in sequence, until isolated communities remain. An external criteria (such as modularity) is used to determine the stopping point of this process. In the dense overlap viewpoint, there is no region with fewer edges, which means that edges at a community boundary never have many paths focused through them. Betweenness is thus unable to determine community boundaries.

## 3. Other algorithms

Thought experiments similar to the above can be performed for other community detection algorithms. While YL claim that existing community detection algorithms can not handle dense overlaps, certain methods can do so. As already explained above, the Absolute Potts Model is able to detect sparse overlaps[38]. Furthermore, other various local optimization algorithms are able to detect communities in the face of dense overlaps[51, 52].

### Appendix C: F-score partition similarity metric

In order to be able to quantify the performance of community detection algorithms, we must have tools to compare the similarity two partitions (or more generally, *covers*) which allow overlaps). Furthermore, one of the core tenants of our multi-resolution algorithm is that high uniformity across replicas indicates good community detection solutions. There are a variety of these functions derived from information theory which answer the question “if you know one partition of the system, what is known about replicas?”.

This F-score development discussed here has certain advantages. First, it can handle overlapping communities. It also can handle incomplete partitions, where the communities being detected or sought consist of only a portion of the nodes of the entire graph, as opposed to other functions which only compare complete partitions of the graph. Thus, the F-score is a valuable tool for local community detection study. The F-score has the interpretation:  $F = 1$  implies that we have exactly recovered a known community, with every node detected and no extraneous nodes detected.

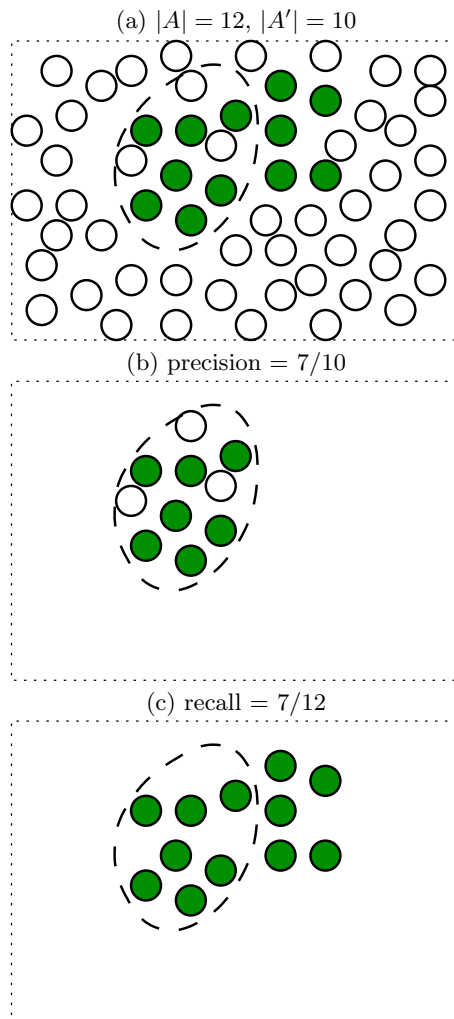


FIG. 9: Example for calculation of F-score. (a) We have a known community  $A$  (green nodes), and the results from the community detection algorithm  $A'$  overlaid (dashed oval). (b) Calculation of precision:  $7/10$  detected nodes are correct. (c) Calculation of recall:  $7/12$  correct nodes are detected.

### 1. Single-community F-score

As an example, let us consider the situation depicted in Fig. 9. We have a community  $A$  which we want to detect. We apply some algorithm and end up with a group of nodes  $A'$  (dark and green). We see there are 10 nodes in  $A$ ,  $|A| = 10$ . Our algorithm has returned 12 nodes,  $|A'| = 12$ . Note that we have an overlap of seven nodes, which means five nodes were detected which are incorrect, and we missed three nodes we should have detected.

We will consider our initial development to be for a single community (in other contexts, F-score is defined only for single-group searching). Using some local community detection algorithm, we detect a group of nodes. We use the phrase “community” to indicate the *known* group of nodes we want to match. We use the term “de-

tected nodes” to indicate what the community detection algorithm actually returns. Note that there are few published local community detection algorithms of this type (that will return only a single community in isolation, as opposed to a partition/cover of the entire system). This is not a practical limitation, as we develop methods of averaging to compensate for this.

There are two components to the F-score. First is the *precision*, measuring how many nodes in the test community actually belong in the known community. It answers the question “of all nodes detected, how many of them are relevant to understanding the characteristic of the community”. Precision is defined

$$\text{precision}(A, A') = \frac{\text{correct nodes returned}}{\text{total nodes returned}} = \frac{|A \cap A'|}{|A'|} \quad (\text{C1})$$

The nomenclature  $|A|$  indicates the number of nodes in  $A$ , and  $\cap$  indicates set intersection. In Fig. 9, precision =  $7/10$ . A precision of 1 indicates that every node detected is in the community. A precision of zero means that no detected nodes are in the community. A lower precision indicates more false positives.

Next, the *recall* indicates what fraction of the community nodes were actually detected. It answers the question “of all nodes in the community (that we want to detect), what fraction were detected?” Recall is defined as

$$\text{recall}(A, A') = \frac{\text{correct nodes returned}}{\text{total community nodes}} = \frac{|A \cap A'|}{|A|} \quad (\text{C2})$$

In Fig. 9, recall =  $7/12$ . A recall of 1 indicates that we have managed to not miss any nodes in the desired community (though there could be excess nodes returned, too). A recall of less than one indicates false negatives.

Generally, there is a trade-off between precision and recall. Precision can be made 1 by selecting fewer nodes (in the limiting case, by selecting only one node which is known to be in the community), at the cost of a very low recall. Conversely, recall can be made 1 by selecting every node in the graph, at the expense of a low precision. Overall goodness of our search process is measured in the form of the *F-score*, the weighted harmonic mean of precision and recall

$$F_\beta(A, A') = (1 + \beta^2) \frac{\text{prec}(A, A') \text{recall}(A, A')}{\beta^2 \text{prec}(A, A') + \text{recall}(A, A')}. \quad (\text{C3})$$

The parameter  $\beta$  weights the relative importance of precision and recall, with a higher  $\beta$  weighting recall more. This selectivity has a benefit in community detection work: if the user has a preference for ensuring detection of all nodes at a possible cost of false positives, or the converse, that can be accommodated.

In our work, we will use  $F_1$ , the balanced score.  $F_1$  is the harmonic mean of precision and recall,

$$F_1(A, A') = 2 \frac{\text{prec}(A, A') \text{recall}(A, A')}{\text{prec}(A, A') + \text{recall}(A, A')}. \quad (\text{C4})$$

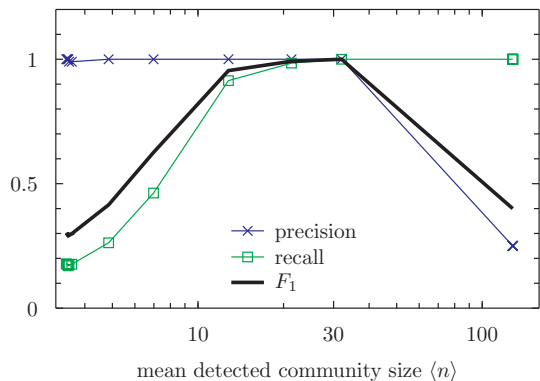


FIG. 10: Trade-off between precision and recall. At low mean community size  $n$ , our detected communities are too small and we have high precision but low recall. At larger community size, our detected communities are too large and we have low precision but high recall. When we properly detect the correct communities, both precision and recall are high, and we have  $F_1 = 1$ . In this sample graph, actual communities have a size of  $n = 32$  which we can observe from the peak of  $F_1$ . This figure actually plots  $F_1^0$  which will be explained in the next sections, but conceptually the results are the same. Tested on  $q = 4$   $n = 32$  SBM graph with  $p_{in} = .5$  and  $p_{out} = .1$ .

The use of  $F_1$  is between a set of nodes (the known “community”  $A$ ) and another set (the “detected nodes”,  $A'$ ), and for  $\beta \neq 1$  is non-symmetric in  $A$  and  $A'$ . For  $\beta = 1$ ,  $F_1$  is symmetric, with precision and recall swapping values when  $A$  and  $A'$  are swapped.

The overall F-score in Fig. 9 is  $\frac{2 \cdot \frac{7^2}{7 \cdot 10 + 12}}{\frac{7}{10} + \frac{12}{7}} \approx .64$ . Note that the F-score does *not* depend on the total number of nodes in the graph. This means our F-score scale does not change as we increase the total graph size (at approximately constant community size), providing theoretical advantages for *local* community detection.

## 2. Partition F-score

In order to compare two partitions, we take one partition as the “known” community assignment we want to match ( $\alpha$ ) and another partition as the result from our (now global) community detection algorithm. We take an average of  $F_1$  scores,

$$F_1^P(\alpha, \alpha') = \frac{1}{|\alpha|} \sum_{A \in \alpha} \max_{A' \in \alpha'} (F_1(A, A')) \quad (\text{C5})$$

In words, for every community  $A$  in the known partition, we compute the F-score with all communities  $A'$  in  $\alpha'$  and, and choose the one which maximizes the  $F_1$  with  $A$ . We take the average value of all of these maxima. The number of communities in  $\alpha$  is represented by  $|\alpha|$ .

As defined above,  $F_1^P$  is non-symmetric. In the final value, each community in  $\alpha$  is used at least once as the first argument to  $F_1$ , but the only communities in  $\alpha'$

used as the second argument are those which maximize  $F_1$  to at least one of the communities in  $\alpha$ . There can be communities in  $\alpha'$  which are left unused and do not affect the result.

It is extremely important to understand the non-symmetric nature of  $F_1^P$ . As it is posed above,  $F_1^P$  is a useful metric if every known community is matched by at least one detected community. It answers the question “Is every community detected at least once?”. A distinct question is “does every community in  $\alpha'$  correspond to at least one real community?”. To answer this second question, we swap the roles of  $\alpha$  and  $\alpha'$  in  $F_1^P$  and instead compute  $F_1^P(\alpha', \alpha)$ . Just like precision and recall both have their uses in understanding the community detection process,  $F_1^P(\alpha', \alpha)$  and  $F_1^P(\alpha, \alpha')$  both tell different and useful properties of our minimization: One answers the question “is every community detected at least once?”, the other answers “does every detected community represent a real community?”

Naively,  $F_1^P$  is an  $O(|\alpha||\alpha'|)$  calculation, because we must compare every community in  $\alpha$  to every community in  $\alpha'$ . There is potential for optimization by first generating a list of only overlapping communities. Each actual  $F_1$  evaluation consists only of the operations of set intersection and set cardinality, which can be made efficient.

Analogously, we could define partition precision/recall as

$$\text{prec}^P(\alpha, \alpha') = \frac{1}{|\alpha|} \sum_{A \in \alpha} \max_{A' \in \alpha'} (\text{prec}(A, A')) \quad (\text{C6})$$

$$\text{recall}^P(\alpha, \alpha') = \frac{1}{|\alpha|} \sum_{A \in \alpha} \max_{A' \in \alpha'} (\text{recall}(A, A')). \quad (\text{C7})$$

A low precision generally indicates that communities are being detected too large or too liberally. A low recall generally indicates that communities are being detected too small or too conservatively. This can provide valuable information to monitor the performance of our algorithm. Note that  $F_1^P$  is not commutative with respect to the averaging and the precision/recall,

$$F_1^P \neq 2 \cdot \frac{\text{prec}^P \text{recall}^P}{\text{prec}^P + \text{recall}^P} \quad (\text{C8})$$

### 3. F-score applications

We apply  $F_1^P$  in two ways: first to, compare the uniformity of a handful of replicas (results from community detection applied to the same graph with different initial conditions/random seeds). Second, to compare partitions with a known state. For these, we assume that we have  $r$  replicas  $\alpha_1, \alpha_2, \dots$

First, we can use  $F_1^P$  as a measure of inter-replica uniformity in our multi-resolution algorithm. This takes the place of the variance of information, normalized mutual

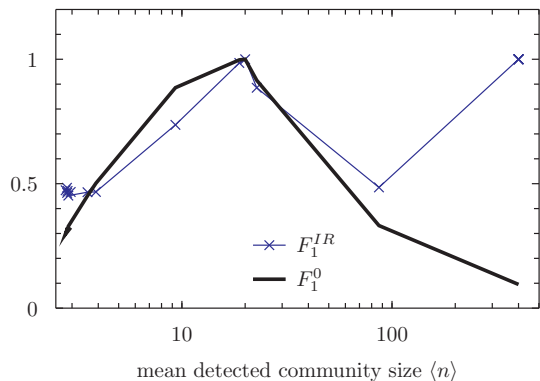


FIG. 11: Comparison between  $F_1^{IR}$  and  $F_1^0$  on a  $q = 20$   $n = 20$  SBM graph. We see that the measures initially reach a maximum at the same point  $n = 20$ , allowing us to use  $F_1^{IR}$  to infer that communities have a size of 20 nodes. The  $n = 400$  maximum of  $F_1^{IR}$  is the trivial result that when one giant community is detected, the result is very uniform.

information, or  $N$ -measure. For this, we calculate  $F_1^P$  with respect to every pair of replicas,

$$F_1^{IR}(\alpha, \beta) = \frac{1}{r-1} \sum_{\alpha \neq \beta} F_1^R(\alpha, \beta), \quad (\text{C9})$$

for the partitions  $\alpha$  and  $\beta$  in the replicas. This measure is 1 when all replicas are identical. Note that we sum over both the argument orders  $(\alpha, \beta)$  and  $(\beta, \alpha)$  due to the non-symmetric nature of the  $F_1^P$  measure.

Next, we can form a version of this measure which detects similarity to a known structure which we designate as  $\alpha_0$ . The  $F_1^P$  score with respect to a known configuration is defined as

$$F_1^0 = \frac{1}{r} \sum_{\alpha} F_1^P(\alpha_0, \alpha) \quad (\text{C10})$$

for all replicas  $\alpha$ . Due to the asymmetric nature of  $F_1^P$ , this measure indicates the extent to which all known communities are detected in replicas, but not the extent to which all detected communities represent real structure. The asymmetric nature of  $F_1$  here is beneficial, because we can handle cases where we partition the entire graph into communities, but can also search for detection of only a few partitions within a larger graph. In Fig. 11, we show that  $F_1^{IR}$  is useful for inferring  $F_1^0$ , and in Fig. 12, we show that  $F_1^P$  behaves similarly to other partition comparison functions.

## 4. Discussion

The F-score is a tool for comparing partitions sharing some similarity with already existing measures, but with the possibility for further extension to local community detection and overlapping nodes. By combining different orders applications of averaging, precisions, recalls, and

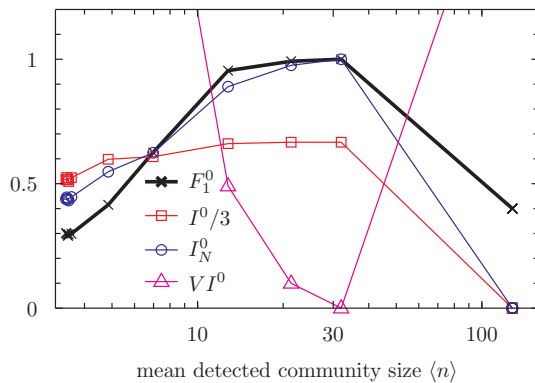


FIG. 12: Comparison of  $F_1^0$  and other partition measures on the same  $q = 4$   $n = 32$  SBM graph. We see that all measures contain extrema at the same community size  $\langle n \rangle$ , validating that all measures convey approximately the same information on this graph. We compare mutual information  $I^0$  [38, 75], normalized mutual information  $I_N$  [38, 75], and variance of information  $VI$  [38, 73, 74].

F-scores, it provides additional insight to the internal workings of CD methods.

- 
- [1] B. Bollobas, *Modern Graph Theory* (Springer Verlag, 1998).
- [2] S. Fortunato, *Physics Reports* **486**, 75 (2010), URL <http://www.sciencedirect.com/science/article/pii/S0370157309002841>.
- [3] J. Yang and J. Leskovec, in *Proceedings of the ACM SIGKDD Workshop on Mining Data Semantics* (ACM, 2012), p. 3, URL <http://dl.acm.org/citation.cfm?id=2350193>.
- [4] A. Mislove, M. Marcon, K. Gummadi, P. Druschel, and B. Bhattacharjee, in *Proceedings of the 7th ACM SIGCOMM conference on Internet measurement* (ACM, 2007), pp. 29–42, URL <http://dl.acm.org/citation.cfm?id=1298311>.
- [5] W. Zachary, *Journal of anthropological research* **33**, 452 (1977), URL <http://www.jstor.org/stable/10.2307/3629752>.
- [6] D. Lusseau, *Proceedings of the Royal Society of London. Series B: Biological Sciences* **270**, S186 (2003), URL [http://rspb.royalsocietypublishing.org/content/270/Suppl\\_2/S186.short](http://rspb.royalsocietypublishing.org/content/270/Suppl_2/S186.short).
- [7] G. Palla, I. Derényi, I. Farkas, and T. Vicsek, *Nature* **435**, 814 (2005), URL <http://www.nature.com/nature/journal/v435/n7043/abs/nature03607.html>.
- [8] R. Prill, P. Iglesias, and A. Levchenko, *PLoS biology* **3**, e343 (2005), URL <http://www.plosbiology.org/article/info%3Adoi%2F10.1371%2Fjournal.pbio.0030343>.
- [9] R. Ferrer i Cancho, C. Janssen, and R. Solé, *Physical Review E* **64**, 046119 (2001), URL <http://link.aps.org/doi/10.1103/PhysRevE.64.046119>.
- [10] K. Calvert, M. Doar, and E. Zegura, *Communications Magazine, IEEE* **35**, 160 (1997), URL [http://ieeexplore.ieee.org/xpls/abs\\_all.jsp?arnumber=587723&tag=1](http://ieeexplore.ieee.org/xpls/abs_all.jsp?arnumber=587723&tag=1).
- [11] F. Radicchi, C. Castellano, F. Cecconi, V. Loreto, and D. Parisi, *Proceedings of the National Academy of Sciences of the United States of America* **101**, 2658 (2004), URL <http://www.pnas.org/content/101/9/2658.short>.
- [12] M. Girvan and M. Newman, *Proceedings of the National Academy of Sciences* **99**, 7821 (2002), URL <http://www.pnas.org/content/99/12/7821.short>.
- [13] M. Newman and M. Girvan, *Physical review E* **69**, 026113 (2004), URL <http://pre.aps.org/abstract/PRE/v69/i2/e026113>.
- [14] M. Newman, *Physical Review E* **69**, 066133 (2004), URL <http://link.aps.org/doi/10.1103/PhysRevE.69.066133>.
- [15] S. Lehmann and L. Hansen, *The European Physical Journal B-Condensed Matter and Complex Systems* **60**, 83 (2007), URL <http://www.springerlink.com/content/p693214864j078v2/>.
- [16] Y. Fan, M. Li, P. Zhang, J. Wu, and Z. Di, *Physica A: Statistical Mechanics and its Applications* **377**, 363 (2007), URL <http://www.sciencedirect.com/science/article/pii/S0378437106012386>.
- [17] S. Fortunato and M. Barthélemy, *Proceedings of the National Academy of Sciences* **104**, 36 (2007), URL <http://www.pnas.org/content/104/1/36.short>.
- [18] A. Lancichinetti and S. Fortunato, *Physical Review E* **84**, 066122 (2011), URL <http://link.aps.org/doi/10.1103/PhysRevE.84.066122>.
- [19] J. Reichardt and S. Bornholdt, *Physical Review E* **74**, 016110 (2006), URL <http://link.aps.org/doi/10.1103/PhysRevE.74.016110>.
- [20] J. Kumpula, J. Saramäki, K. Kaski, and J. Kertesz, *The European Physical Journal B-Condensed Matter and Complex Systems* **56**, 41 (2007), URL <http://www.springerlink.com/content/v814645343243536/>.
- [21] R. Guimera, M. Sales-Pardo, and L. Amaral, *Physical Review E* **70**, 025101 (2004), URL <http://link.aps.org/doi/10.1103/PhysRevE.70.025101>.
- [22] J. Reichardt and S. Bornholdt, *Physical Review Letters* **93**, 218701 (2004), URL <http://prl.aps.org/abstract/PRL/v93/i21/e218701>.

- [23] B. Good, Y. de Montjoye, and A. Clauset, *Physical Review E* **81**, 046106 (2010), URL <http://link.aps.org/doi/10.1103/PhysRevE.81.046106>.
- [24] J. Duch and A. Arenas, *Physical review E* **72**, 027104 (2005), URL <http://link.aps.org/doi/10.1103/PhysRevE.72.027104>.
- [25] J. Hofman and C. Wiggins, *Physical review letters* **100**, 258701 (2008), URL <http://link.aps.org/doi/10.1103/PhysRevLett.100.258701>.
- [26] P. Schuetz and A. Caffisch, *Physical Review E* **77**, 046112 (2008), URL <http://link.aps.org/doi/10.1103/PhysRevE.77.046112>.
- [27] U. Brandes, D. Dellinger, M. Gaertler, R. Gorke, M. Hofer, Z. Nikoloski, and D. Wagner, *Knowledge and Data Engineering, IEEE Transactions on* **20**, 172 (2008), URL [http://ieeexplore.ieee.org/xpls/abs\\_all.jsp?arnumber=4358966](http://ieeexplore.ieee.org/xpls/abs_all.jsp?arnumber=4358966).
- [28] V. Blondel, J. Guillaume, R. Lambiotte, and E. Lefebvre, *Journal of Statistical Mechanics: Theory and Experiment* **2008**, P10008 (2008), URL <http://iopscience.iop.org/1742-5468/2008/10/P10008>.
- [29] J. Pujol, J. Béjar, and J. Delgado, *Physical Review E* **74**, 016107 (2006), URL <http://link.aps.org/doi/10.1103/PhysRevE.74.016107>.
- [30] X. Liu and T. Murata, *Physica A: Statistical Mechanics and its Applications* **389**, 1493 (2010), URL <http://www.sciencedirect.com/science/article/pii/S0378437109010152>.
- [31] A. Noack and R. Rotta, *Experimental Algorithms* pp. 257–268 (2009), URL <http://www.springerlink.com/content/qugv7708h3806230/>.
- [32] G. Agarwal and D. Kempe, *The European Physical Journal B-Condensed Matter and Complex Systems* **66**, 409 (2008), URL <http://www.springerlink.com/content/w3221r727wr20x74/>.
- [33] S. Mancoridis, B. Mitchell, C. Rorres, Y. Chen, and E. Gansner, in *Program Comprehension, 1998. IWPC'98. Proceedings., 6th International Workshop on* (IEEE, 1998), pp. 45–52, URL [http://ieeexplore.ieee.org/xpls/abs\\_all.jsp?arnumber=693283](http://ieeexplore.ieee.org/xpls/abs_all.jsp?arnumber=693283).
- [34] S. Wasserman and K. Faust, *Social Network Analysis* (Cambridge University Press, 1994).
- [35] J. Scott, *Social Network Analysis: A Handbook* (SAGE Publications, 2000).
- [36] J. Moody and D. White, *American Sociological Review* **68**, 103 (2003), URL <http://www.jstor.org/stable/3088904>.
- [37] R. Luce and A. Perry, *Psychometrika* **14**, 95 (1949), URL <http://www.springerlink.com/content/j7u53t8276412qp7/>.
- [38] P. Ronhovde and Z. Nussinov, *Physical Review E* **80**, 016109 (2009), 0812.1072, URL <http://link.aps.org/doi/10.1103/PhysRevE.80.016109>.
- [39] P. Ronhovde and Z. Nussinov, *Physical Review E* **81**, 046114 (2010), URL <http://link.aps.org/doi/10.1103/PhysRevE.81.046114>.
- [40] J. Yang and J. Leskovec, *Arxiv preprint arXiv:1205.6228* (2012), URL <http://arxiv.org/abs/1205.6228>.
- [41] A. Condon and R. Karp, *Random Structures and Algorithms* **18**, 116 (2001), URL <http://onlinelibrary.wiley.com/doi/10.1002/1098-2418%28200103%2918:2%3C116::AID-RSA1001%3E3.0.CO;2-2/abstract>.
- [42] F. Wu, *Reviews of modern physics* **54**, 235 (1982), URL <http://link.aps.org/doi/10.1103/RevModPhys.54.235>.
- [43] R. B. Potts and C. Domb, in *Proceedings of the Cambridge Philosophical Society* (1952), vol. 48, p. 106, URL <http://dx.doi.org/10.1017%2FS0305004100027419>.
- [44] J. Ashkin and E. Teller, *Phys. Rev.* **64**, 178 (1943), URL <http://dx.doi.org/10.1103%2FPhysRev.64.178>.
- [45] T. Heimo, J. Kumpula, K. Kaski, and J. Saramäki, *Journal of Statistical Mechanics: Theory and Experiment* **2008**, P08007 (2008), URL <http://iopscience.iop.org/1742-5468/2008/08/P08007>.
- [46] A. Lancichinetti and S. Fortunato, *Physical Review E* **80**, 056117 (2009), URL <http://link.aps.org/doi/10.1103/PhysRevE.80.056117>.
- [47] P. Ronhovde, S. Chakrabarty, D. Hu, M. Sahu, K. Sahu, K. Kelton, N. Mauro, and Z. Nussinov, *The European Physical Journal E: Soft Matter and Biological Physics* **34**, 1 (2011), URL <http://link.springer.com/article/10.1140/epje/i2011-11105-9>.
- [48] V. Traag, P. Van Dooren, and Y. Nesterov, *Physical Review E* **84**, 016114 (2011), URL <http://link.aps.org/doi/10.1103/PhysRevE.84.016114>.
- [49] D. Hu, P. Ronhovde, and Z. Nussinov, *Philosophical Magazine* **92**, 406 (2011), URL <http://www.tandfonline.com/doi/abs/10.1080/14786435.2011.616547>.
- [50] D. Hu, P. Ronhovde, and Z. Nussinov, *Phys. Rev. E* **85**, 016101 (2012), URL <http://link.aps.org/doi/10.1103/PhysRevE.85.016101>.
- [51] A. Lancichinetti, S. Fortunato, and J. Kertész, *New Journal of Physics* **11**, 033015 (2009), URL <http://iopscience.iop.org/1367-2630/11/3/033015>.
- [52] A. Lancichinetti, F. Radicchi, J. Ramasco, and S. Fortunato, *PLoS One* **6**, e18961 (2011), URL <http://www.plosone.org/article/info%3Adoi%2F10.1371%2Fjournal.pone.0018961>.
- [53] C. Lee, F. Reid, A. McDaid, and N. Hurley, *Arxiv preprint arXiv:1002.1827* (2010), URL <http://arxiv.org/abs/1002.1827>.
- [54] G. Simmel, *Conflict and the web of group affiliations* (Free Pr, 1964).
- [55] S. Feld, *American journal of sociology* **86**, 1015 (1981), URL <http://www.jstor.org/stable/2778746>.
- [56] Y. Ahn, J. Bagrow, and S. Lehmann, *Nature* **466**, 761 (2010), URL <http://www.nature.com/nature/journal/v466/n7307/abs/nature09182.html>.
- [57] A. Lancichinetti and S. Fortunato, *Phys. Rev. E* **80**, 016118 (2009), URL <http://link.aps.org/doi/10.1103/PhysRevE.80.016118>.
- [58] R. Breiger, *Social forces* **53**, 181 (1974), URL <http://sf.oxfordjournals.org/content/53/2/181.short>.
- [59] M. Newman, *SIAM review* **45**, 167 (2003), URL <http://www.jstor.org/stable/10.2307/25054401>.
- [60] R. Darst, D. Reichman, P. Ronhovde, and Z. Nussinov, to be submitted.
- [61] R. Guimerà, L. Danon, A. Díaz-Guilera, F. Giralt, and A. Arenas, *Phys. Rev. E* **68**, 065103(R) (2003), URL <http://link.aps.org/doi/10.1103/PhysRevE.68.065103>.
- [62] A. Clauset, M. Newman, and C. Moore, *Physical review E* **70**, 066111 (2004), URL <http://link.aps.org/doi/10.1103/PhysRevE.70.066111>.
- [63] S. Boccaletti, V. Latora, Y. Moreno, M. Chavez, and D. Hwang, *Physics reports* **424**, 175 (2006), URL <http://www.sciencedirect.com/science/article/>

- pii/S037015730500462X.
- [64] R. Albert, H. Jeong, and A.-L. Barabási, *Nature* **401**, 130 (1999), URL <http://www.nature.com/nature/journal/v401/n6749/full/401130a0.html>.
- [65] A. Barabási and R. Albert, *science* **286**, 509 (1999), URL <http://www.sciencemag.org/content/286/5439/509.short>.
- [66] S. Lattanzi and D. Sivakuma, in *Proceedings of the 41st annual ACM symposium on Theory of computing* (ACM, 2009), pp. 427–434, URL <http://dl.acm.org/citation.cfm?id=1536414.1536474>.
- [67] P. Ronhovde and Z. Nussinov, Arxiv preprint arXiv:1208.5052 (2012), URL <http://arxiv.org/abs/1208.5052>.
- [68] Unpublished, Z. Nussinov, P. Ronhovde, D. Hu.
- [69] A. Arenas, A. Fernandez, and S. Gomez, *New Journal of Physics* **10**, 053039 (2008), URL <http://iopscience.iop.org/1367-2630/10/5/053039>.
- [70] A. Traud, E. Kelsic, P. Mucha, and M. Porter, *SIAM Review* **53**, 526 (2008), URL <http://dx.doi.org/10.1137/080734315>.
- [71] D. MacKay, *Information Theory, Inference, and Learning Algorithms* (Cambridge: Cambridge University Press, 2002).
- [72] M. Rosvall and C. Bergstrom, *Proceedings of the National Academy of Sciences* **104**, 7327 (2007), URL <http://www.pnas.org/content/104/18/7327.short>.
- [73] B. Karrer, E. Levina, and M. Newman, *Physical Review E* **77**, 046119 (2008), URL <http://link.aps.org/doi/10.1103/PhysRevE.77.046119>.
- [74] M. Meilă, *Journal of Multivariate Analysis* **98**, 873 (2007), URL <http://dx.doi.org/10.1016/j.jmva.2006.11.013>.
- [75] L. Danon, A. Diaz-Guilera, J. Duch, and A. Arenas, *Journal of Statistical Mechanics: Theory and Experiment* **2005**, P09008 (2005), URL <http://dx.doi.org/10.1088/1742-5468/2005/09/P09008>.